water

MDPI

Article

Coupling Microalgae Cultivation in Mine Wastewater with Soil Restoration in Coal Mine Spoil Heaps

Peng Yu [1,2], Bo Huang [3], Jinli Zhang [3], Xufan Zheng [2], Zhikun Xin [2], Tao Tang [3], Rui Zhao [2], Dong Xu [2], Yuke Hu [3,*] and Keqing Li [1,*]

[1] School of Resources and Safety Engineering, University of Science and Technology Beijing, Beijing 100083, China; 20001539@ceic.com
[2] ChnEnergy New Energy Technology Research Institute Co., Ltd., Beijing 102211, China; 20082056@ceic.com (X.Z.); 20082057@ceic.com (Z.X.); 16810096@ceic.com (R.Z.); 12000185@ceic.com (D.X.)
[3] State Key Laboratory of Low Carbon Catalysis and Carbon Dioxide Utilization, Shanghai Advanced Research Institute, Chinese Academy of Sciences, Shanghai 201210, China; huangb@sari.ac.cn (B.H.); zhangjinli@sari.ac.cn (J.Z.); tangt@sari.ac.cn (T.T.)
* Correspondence: huyk@sari.ac.cn (Y.H.); likeqing@ustb.edu.cn (K.L.)

Abstract

Open-pit coal mining has created spoil dumps with poor soil structure and nutrient deficiency, challenging ecological restoration. This study developed a low-cost integrated remediation strategy combining microalgae, organic fertilizer, and cold- and drought-tolerant plants. First, local mine water was evaluated for microalgae cultivation. HS5 grew best in untreated mine water supplemented with partial BG11, a 0.1 g L^{-1} inoculation density, and 25–50 μmol m^{-2} s^{-1} light. Then, a 90-day field experiment was conducted, which included a control (CK), microalgae (M), organic fertilizer (F), and combined microalgae + organic fertilizer (MF), all sown with Dahurian wildrye and sainfoin. Compared with the CK, the M and F, both alone and combined, promoted plant growth and improved the soil properties, with the MF performing best. Compared with the CK, the MF significantly increased the total nitrogen content by 107.4%, soil organic matter by 89.5%, and available phosphorus by 52.7%, and raised the fresh and dry weights of both plants by 759.4–1084.2% and 660.6–891.7%, respectively. The MF also enriched the beneficial bacterial phyla, such as *Bacillota* and *Bacteroidota*, while reducing *Acidobacteriota*. These findings indicate that mine water-based microalgae cultivation is feasible, and that a microalgae–organic fertilizer–herbaceous plants system is a promising low-cost and sustainable strategy for restoring coal mine spoil dumps.

Keywords: open-pit coal mine; mine wastewater utilization; microalgae cultivation; soil restoration

Check for updates

Academic Editor: Christos S. Akratos

Received: 3 October 2026
Revised: 5 November 2026
Accepted: 5 November 2026
Published: 9 November 2026

Copyright: © 2026 by the authors. Licensee MDPI, Basel, Switzerland. This article is an open access article distributed under the terms and conditions of the Creative Commons Attribution (CC BY) license.

1. Introduction

Open-pit coal mining and associated dumping operations have led to extensive land degradation, particularly in arid and semi-arid regions [1,2]. The soils in these mine spoil heaps commonly suffer from low organic matter content, nutrient deficiency, high pH or salinization, and poor water and nutrient retention capacity [3–5]. In the Xinjiang Uygur Autonomous Region of China, the Heishan Coal Mine, a representative open-pit mine located in a cold, high-altitude, arid zone, is characterized by intense solar radiation, scarce precipitation, strong winds, and a short growing season, all of which collectively constrain the ecological restoration of coal mine spoil heaps [6]. Therefore, developing low-cost

restoration technologies that are well adapted to local environmental conditions is of great significance for achieving sustainable rehabilitation of coal mine spoil heaps [7].

Current soil remediation techniques for mining areas can be broadly classified into three categories: physical, chemical, and biological remediation [8,9]. Physical and chemical amendments may produce relatively quick improvements in soil physicochemical properties, but these improvements are often temporary, and such methods alone generally fail to restore a complete, self-sustaining soil ecosystem in the long term [10–13]. In contrast, bioremediation has become an important approach for mine site restoration due to its environmental friendliness, non-polluting nature, and relatively low cost [14,15]. However, under the constraints of harsh natural environments, poor soil structure, and severe nutrient depletion, these methods face significant practical limitations. Sole reliance on revegetation often results in low seedling survival and slow growth due to insufficient nutrients and water, while single bacterial inoculation frequently leads to poor colonization and rapid functional decline owing to the lack of organic substrates and suitable microhabitats [16]. Consequently, there is an urgent need to integrate multiple remediation approaches, leveraging their respective advantages and compensating for each other's weaknesses, to form a synergistic comprehensive restoration strategy capable of addressing the complex challenges of ecological restoration in cold and arid open-pit coal mine dumps [17].

Microalgae, particularly nitrogen-fixing cyanobacteria, play a pivotal role as pioneer organisms in desertified soil restoration, owing to their strong environmental adaptability, high photosynthetic activity, and rapid reproduction rates [18,19]. Nitrogen-fixing cyanobacteria can survive and proliferate under extreme drought, intense light, and large temperature fluctuations through stress resistance mechanisms, such as akinete formation and protective pigments [20,21]. During their growth, they convert atmospheric CO_2 and N_2 into organic carbon and nitrogen, thereby enhancing soil carbon and nitrogen pools [22,23]. Additionally, they increase plant-available phosphorus and potassium levels through phosphate solubilization and potassium mobilization [24–26]. Cyanobacteria also secrete phytohormone-like substances that enhance plant stress tolerance and growth performance [27,28]. Most importantly, through the mechanical entanglement of filamentous cells and the secretion of large amounts of extracellular polymeric substances (EPSs), they improve soil aggregate stability, form stable biological soil crusts, reduce evaporation, intercept condensate water, and ultimately enhance soil water and nutrient retention capacity [29–32]. These attributes make them particularly suitable for restoring mine dumps with harsh environmental conditions and low soil nutrient content.

However, large-scale cultivation of microalgae requires not only substantial CO_2 but also significant inputs of nitrogen, phosphorus, and trace elements to sustain normal growth and metabolism, while the entire cultivation process consumes considerable freshwater resources [33,34]. Under the extremely water-scarce conditions of northwestern China, this requirement limits the widespread application of microalgae-based ecological restoration technologies. Notably, coal mining operations in this region generate large volumes of mine water, which can serve as an alternative water source for large-scale microalgae cultivation. Moreover, mine water typically contains dissolved inorganic salts, trace metal elements and, in some cases, nitrogen and phosphorus nutrients, which can partially reduce the demand for exogenous nutrients in microalgae cultivation [35–37]. Nevertheless, systematic studies on the effects of mine water from cold and arid open-pit coal mines on the growth and physiological activity of nitrogen-fixing cyanobacteria remain lacking.

Dahurian wildrye (*E. dahuricus*), a cold- and drought-tolerant perennial grass, is widely used in mine site restoration across northern and northwestern China due to its rapid establishment, high biomass production, and strong root system for soil stabilization [38–40]. The fibrous roots of Dahurian wildrye are fine and dense, with numerous branches that

intertwine and penetrate the surface soil, forming a three-dimensional 'reinforcing network'. Soil containing Dahurian wildrye root systems exhibits a significant increase in shear strength, with an improvement of approximately 23% [41]. As a legume, sainfoin (*O. viciifolia*) employs rhizobium bacteria to fix nitrogen biologically, converting atmospheric nitrogen into a form that can be utilized by plants. While supporting its own growth, this nitrogen can be supplied in a slow-release manner to Dahurian wildrye and rhizosphere microorganisms, providing a continuous nitrogen source for the entire mixed-sowing system [42,43]. Chemical fertilizers can rapidly alleviate nutrient deficiency in mine soils, but their benefits are short-lived and they supply neither organic carbon nor suitable microhabitats. Organic fertilizers and microalgae are therefore applied together: the organic fertilizer provides a resource-rich substrate and microbial base, while microalgae confer the decisive early-stage advantage by fixing carbon in situ, secreting EPSs that bind soil particles, and stabilizing the surface and promoting biocrust formation before the added organic matter is fully incorporated [44–46]. In this study, we propose a combined remediation strategy integrating sainfoin and Dahurian wildrye, organic fertilizer, and nitrogen-fixing cyanobacteria for mine soil restoration. Within this system, Dahurian wildrye provides aboveground vegetation cover and belowground root reinforcement. Sainfoin with rhizobium bacteria fixes nitrogen from the atmosphere. Organic fertilizer supplies a subsurface nutrient reservoir and microbial substrate, and cyanobacteria contribute surface biological crust protection along with sustained biological nitrogen fixation and carbon sequestration. The synergistic interaction among these three components is expected to establish a three-dimensional remediation framework, namely crust formation for surface stabilization, organic amendment for soil fertility improvement, and vegetation establishment, thereby overcoming the limitations of individual techniques.

This study takes the Heishan Coal Mine spoil heaps in Xinjiang as the research object and systematically investigates the following aspects. First, it evaluates the feasibility of cultivating nitrogen-fixing cyanobacteria using mine water and optimizes the cultivation conditions. On this basis, it examines the synergistic effects of combined application of nitrogen-fixing cyanobacteria, organic fertilizer, sainfoin and Dahurian wildrye on the soil physicochemical properties, nutrient status, microbial community structure, and vegetation restoration performance in mine dumps, and further elucidates the key driving mechanisms underlying the cyanobacteria–organic fertilizer–grass–combined remediation approach. This study aims to provide theoretical foundations and technical support for low-cost, sustainable ecological restoration of open-pit coal mine spoil heaps in cold and arid regions.

2. Materials and Methods

2.1. Experimental Setup and Cultivation Conditions of Mine Water

2.1.1. Experimental Cyanobacterial Strains and Mine Water

The mine water was sourced from the Heishan Coal Mine in Toksun County, Xinjiang, China. As shown in Table S1, the mine water is weakly alkaline in nature. Two types of water were used: raw mine water (XJ0) and flocculated water (XJ1). The XJ0 contained 0.078 mg L^{-1} of arsenic, 16.3 μg L^{-1} of selenium, 0.804 mg L^{-1} of manganese, 15.0 mg L^{-1} of iron, and 0.164 mg L^{-1} of chromium. Flocculation was achieved by adding 0.1 g L^{-1} of polyacrylamide to the raw water based on the dosage used on-site at the Heishan Coal Mine. The XJ1 showed a slightly higher total hardness, total soluble solids and SO_4^{2-} than the XJ0, perhaps because some of the polyacrylamide that was added underwent hydrolysis, which in turn promoted the dissolution of insoluble calcium and magnesium in the water. The free polymers that did not participate in the flocculation remained in the water, thereby increasing the content of soluble solids. Five microalgae strains were used, all isolated from local soil samples at the Heishan Coal Mine: HS1–HS5. Inside a laminar flow

hood, 2 g of soil from the Heishan Coal Mine was weighed and added to Erlenmeyer flasks containing 80 mL of sterilized BG11 medium and $BG11_0$ medium, respectively. The flasks were sealed with sealing film and incubated on an orbital shaker at 160 rpm, 25 °C, and 100 μmol m^{-2} s^{-1}. The microalgal cells grown in the suspensions were then isolated and purified, yielding the HS1–HS5 algal strains. HS1–2 were isolated from BG11 and HS3–5 were isolated from $BG11_0$. Pre-culture was performed in bubble column photobioreactors with 1% CO_2 at 100 μmol m^{-2} s^{-1} and 25 °C. Cells were harvested during the logarithmic growth phase by centrifugation.

2.1.2. Experimental Setup for Microalgae Cultivation Using Mine Water

The microalgae were cultured directly in mine water medium. The experiments investigated the effects of: (1) water type (XJ0, XJ1), (2) inoculation concentration (0.05, 0.1, and 0.2 g L^{-1}), (3) medium composition ratio (XJ0 diluted with $BG11_0$ culture medium to ratios of 1:0 (HS-O), 1:1 (HS-H), and 1:3 (HS-Q)), and (4) light intensity (25, 50, and 100 μmol m^{-2} s^{-1}). The culture parameters for different experimental conditions are shown in Table S2. Cultivation was carried out in 100 mL conical flasks (80 mL working volume) at 25 °C and 150 rpm min^{-1} in a laboratory shaker. Samples were taken every two days for analysis. Microscopic observation was conducted at the final sampling point using an Olympus microscope (Olympus BX53, Olympus Corporation, Tokyo, Japan).

2.1.3. Analytical Methods

The pH was measured by using a pH meter (Mettler Toledo, Zurich, Switzerland). The dry weight of microalgae (DW) was measured by filtering a 5 mL aliquot of the culture through pre-weighed Whatman GF/C filter paper (0.22 μm, Titan, Shanghai, China). The filter papers were dried at 105 °C in a vacuum oven until constant weight and were subsequently cooled down to room temperature in a desiccator before weighing. The chlorophyll content was determined by an ethanol–acetone extraction method according to the agricultural industry standard of China (NY–T 3082–2017) [47], and the maximum chlorophyll fluorescence quantum yield (F_v/F_m) were determined by a Hansatech Fluorescence Monitoring System (FMS–2, Hansatech Instruments Ltd., Norfolk, UK).

2.2. Field Experiment on Ecological Restoration with Microalgae Biomass

2.2.1. Experimental Site

The experimental location was the Heishan Coal Mine in Toksun County, Xinjiang, China. The climate is characterized by a continental arid and subarctic climate. The average elevation is over 2200 m. The average annual temperature is 1.2–2.3 °C. The average annual precipitation and evaporation are 150–160 mm and 1100–2100 mm, respectively. During the 90–day experimental period, the average temperature in this region ranged from 26 to 40 °C, the average humidity was 30–40%, and the total precipitation was 51.3 mm. The soil had an organic matter content (SOM) of 7.64 g kg^{-1}, total nitrogen content (TN) of 0.26 g kg^{-1}, alkaline-hydrolyzable nitrogen content (AHN) of 12.01 mg kg^{-1}, total phosphorus content (TP) of 0.21 g kg^{-1}, available phosphorus content (AP) of 1.46 mg kg^{-1}, total potassium content (TK) of 8.27 g kg^{-1}, available potassium content (AK) of 85.58 mg kg^{-1} and electrical conductivity (EC) of 8.23 mS m^{-1}. The soil showed a pH of 8.84 (soil:water = 1:2.5).

2.2.2. Experimental Design

The total area of the experimental plot was approximately 500 m^2, divided into 12 equal-sized subplots, each measuring approximately 42.5 m^2. The experiment consisted of 4 treatments, each with 3 replicates: (1) a control group receiving no treatment (CK); (2) microalgae treatment (M); (3) organic fertilizer treatment (F); and (4) microalgae + organic

fertilizer treatment (MF). The diagram of experimental site division is shown in Figure S1. Through laboratory pot experiments, the effects of microalgae application rates on soil nutrients and the growth of Dahurian wildrye and sainfoin were investigated (unpublished data), and the optimal dosage of the microalgae was determined to be 1.5 g m^{-2} (in dry weight). The organic fertilizer used in this experiment was provided by Shenyang Agricultural University, and the dosage of organic fertilizer was 6 kg m^{-2}. The raw materials for the organic fertilizer were hay and animal manure collected from the soil restoration area. The raw materials were crushed and mixed with a microbial inoculant, fermented at 50–60 °C for 30 days, and then naturally cooled before use. The main parameters of the organic fertilizer were pH = 6.7, 456 g kg^{-1} organic matter, 16.5 g kg^{-1} total nitrogen, 6.1 g kg^{-1} total phosphorus and 20.8 g kg^{-1} total potassium.

The plants used in this experiment were Dahurian wildrye and sainfoin, which were sown as a mixture, with a total seeding rate of 15 g m^{-2}, comprising 13 g m^{-2} of Dahurian wildrye and 2 g m^{-2} of sainfoin. The organic fertilizer was evenly broadcast, and the top 20 cm of soil was then tilled with a rotary tiller to ensure thorough mixing of the fertilizer with the soil. Then, seeds were uniformly broadcast, and the covered soil was lightly raked. Subsequently, microalgae were inoculated. Algal cultures grown to the logarithmic growth phase were uniformly sprayed onto the surface of the soil to be remediated using a manual sprayer.

During the week before sowing, the plots were watered daily at approximately 0.25 L m^{-2}. After the application of organic fertilizer, the first sprinkler irrigation was performed using a high-pressure water gun, with an irrigation amount of approximately 15 L m^{-2}. A second irrigation was conducted after 15 days, with the same irrigation amount and method as the first irrigation. One month later, a third irrigation was carried out using the same irrigation amount and method as the previous two irrigations. Subsequently, the plots were watered daily with a watering can at approximately 0.25 L m^{-2}.

2.2.3. Sampling and Measurements

At 45 and 90 days, soil samples were collected from the 0–20 cm plough layer using a five-point sampling method, and the subsamples were thoroughly mixed for the analysis of soil physicochemical properties. Soil pH was measured using a pH meter at a soil/distilled water ratio of 1:2.5 [48], and EC was measured using a conductivity meter at a soil/distilled water ratio of 1:5 [49]. Soil organic carbon content was measured using the Springer-Klee method [50] and converted to SOM using the van Bemmelen factor [51]. TN was measured using the Kjeldahl method [52], AHN was measured using the method of Roberts et al. [53], TP was measured using the alkali fusion–Mo-Sb anti-spectrophotometric method [54], and AP was measured using the sodium hydrogen carbonate solution–Mo-Sb anti-spectrophotometric method [55].

At 90 days, Dahurian wildrye and sainfoin were collected by a five-point sampling method. The plant height (PH) and root length (RL) were measured using a tape measure. The samples were rinsed thoroughly, blotted to remove surface water, and weighed to determine the fresh weight (FW). Then, the samples were oven-dried at 105 °C for 30 min, followed by drying at 75 °C to a constant weight, and weighed to determine the dry weight (DW).

The surface soils were collected at 90 days. The soil microbial diversity assessment was organized through PCR amplification, DNA extraction and high-throughput gene sequencing. A blank control was used during PCR amplification. The soil microbial DNA was extracted using a DNA extraction kit (Shanghai Major Yuhua, Shanghai, China). The quality of DNA was measured by 1% (w/v) agarose gel, and the concentration and purity of DNA were measured using a NanoDrop2000 (Thermo Fisher Scientific, Carlsbad, CA,

USA). The V3-V4 variable regions of 16S rRNA genes were amplified using primers 338F (5′-ACTCCTACGGGAGGCAGCAG-3′) and 806R (5′-GGACTACHVGGGTWTCTAAT-3′), and a 2% (w/v) agarose gel was used for verification. Sequencing was conducted using an Illumina PE300 (Shanghai Majorbio, Shanghai, China). The operational taxonomic units (OTUs) were clustered based on non-repetitive sequences (excluding single sequences) with a 97% similarity threshold. Because the soil in coal mine heaps is characterized by low biomass, 97% OTUs clustering was used. Data was analyzed using Majorbio Isanger Cloud platform (Shanghai Majorbio, Shanghai, China).

2.3. Data Analysis

Data processing was carried out using Microsoft Excel 365. Statistical analysis was carried out using IBM SPSS Statistics 27. Figures were generated using Origin 2019. One-way ANOVA was used to assess differences among treatments, and Levene's test was conducted to verify homogeneity of variances ($p > 0.05$). When significant differences were observed, LSD tests were employed for multiple comparisons ($p \leq 0.05$).

3. Results

3.1. The Impacts of Mine Water and Environmental Factors on Microalgae Cultivation

3.1.1. The Impacts of Different Types of Mine Water

To identify the suitable mine water type and algal strains, we investigated the effects of raw mine water (XJ0) and flocculated mine water (XJ1) on the growth of five microalgal strains. As shown in Figure S2A, the color of algal suspensions gradually changed from blue-green to yellow-green over cultivation, with similar color profiles between the XJ0 and XJ1 groups. HS4 and HS5 maintained long, intact blue-green filaments, and they exhibited better morphological integrity and pigment deposition in the raw mine water than in the flocculated mine water (Figure S2B).

Figure 1 presents the temporal variations in pH, maximum PSII quantum yield (F_v/F_m), dry weight (DW), and chlorophyll a (Chl a) of five strains (HS1–HS5) cultured in XJ0 or XJ1 for six days. The pH rose from 8.5 to 11 across all treatments. Naturally alkaline coal mine water, rich in bicarbonate, favors inorganic carbon utilization by photoautotrophs. The XJ1 treatments generally had a higher pH than the XJ0, indicating superior photosynthetic activity of microalgae in raw mine water. Among the strains, HS4 and HS5 yielded significantly higher pH values than HS1–HS3. The F_v/F_m ranged from 0.2 to 0.6 and declined over time. Relatively high values persisted from day 2 to day 4, followed by sharp decreases on day 6 for all groups. The dry weight increased steadily (0.3–1.1 g L^{-1}), with XJ0-HS5 obtaining the maximum final biomass, which reflected the combined advantages of low turbidity and strain-specific tolerance. The biomass of XJ1-HS1 in our study agrees with the published data for mine water-cultivated cyanobacteria. The Chl a content varied greatly (0.3–4 mg L^{-1}), and was significantly influenced by both the mine water type and strain. XJ0-HS5 had the highest Chl a from day 4 to day 6, demonstrating strong photosynthetic capacity, whereas the XJ1 and sensitive strains (HS1HS3) showed poor Chl a accumulation. In the later phase, the DW and Chl a were decoupled: DW kept increasing while Chl a plateaued or decreased.

The combination of untreated raw mine water (XJ0) with strains HS4 and HS5 represented the optimal system, balancing efficient light utilization and sufficient nutrient supply. This combination was therefore selected as the experimental material for subsequent experiments.

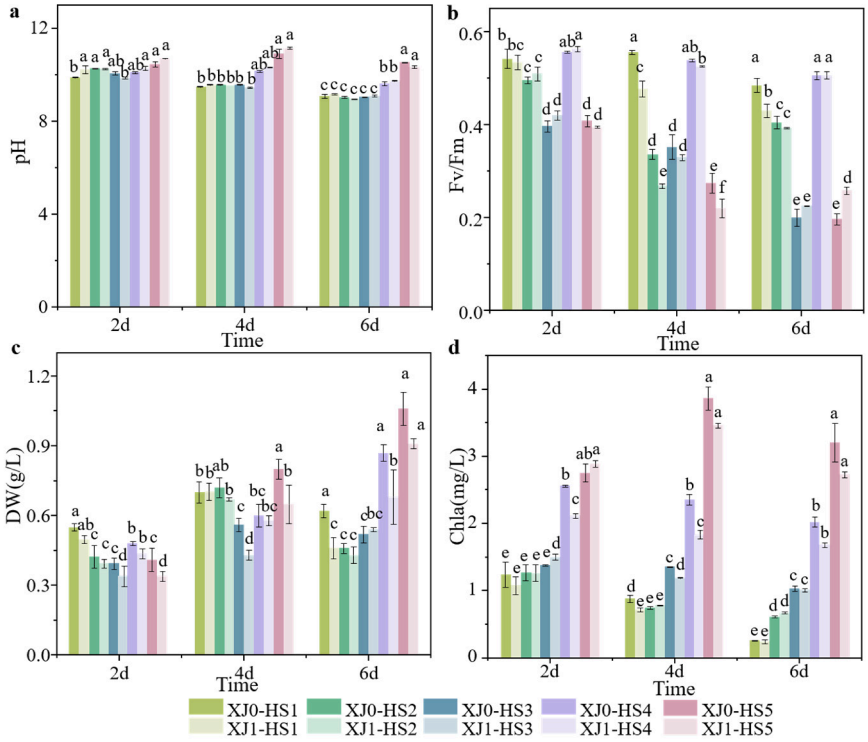


Figure 1. Changes in pH (**a**), F_v/F_m (**b**), DW (**c**) and chlorophyll (**d**) in different treatments. Numbers 15 represent different microalgae; XJ0 is raw water and XJ1 is flocculated water. Error bars represent the standard errors of the triplicate bottles. The different letters above the columns indicate a significant difference ($p < 0.05$) based on the analysis of variance.

3.1.2. The Impacts of Initial Biomass Concentration

Building on the findings from the previous Section 3.1.1, where raw water supported better physiological activity compared to flocculated water, and HS4 and HS5 demonstrated greater adaptability, this section examines the effect of initial biomass concentration (inoculum density) on microalgal growth. This parameter plays a fundamental role in establishing the initial conditions of culture growth and can significantly affect the dynamics of all growth phases from lag to stationary. Representative experimental and microscopic images are provided in Figure S3. The visual and microscopic inspection indicated that HS5-0.1 maintained a comparatively better physiological state.

Figure 2 shows temporal changes in strains HS4 and HS5 cultured for six days at three initial inoculum densities (0.05, 0.1, and 0.2). No day 6 measurements were collected for HS4-0.2 due to severe algal mortality. Across all treatments, pH rose from approximately 9.0–10.0 (day 2) to 10.0–11.5 (day 6). HS5 generally yielded higher pH than HS4, and the highest-density groups (HS4-0.2, HS5-0.2) consistently maintained maximum pH (Figure 2a). F_v/F_m ranged from 0.15 to 0.55 and declined over time. HS4 retained relatively high F_v/F_m (approximately 0.5–0.55) on day 2, whereas HS5-0.2 reached only around 0.35. Sharp F_v/F_m drops occurred on days 46, especially under 0.2 inoculum density. Dry weight increased steadily in most groups from day 2 to day 6. By contrast, HS4-0.2 peaked on day 2 and then declined rapidly, with HS4-0.1 surpassing it on day 4. On day 6, HS5-0.2 reached its maximum dry weight value, while the lowest inoculum density (0.05) generally produced the lowest final biomass. Chl a concentrations varied widely (0.55.0 mg L^{-1}) and diverged from dry weight trends. HS4-0.2 exhibited an extremely high Chl a peak (around 5.0 mg L^{-1}) on day 2, followed by a gradual decrease. In comparison, HS5-0.2 displayed a continuous upward trend and attained approximately 3.2 mg L^{-1} at day 6.

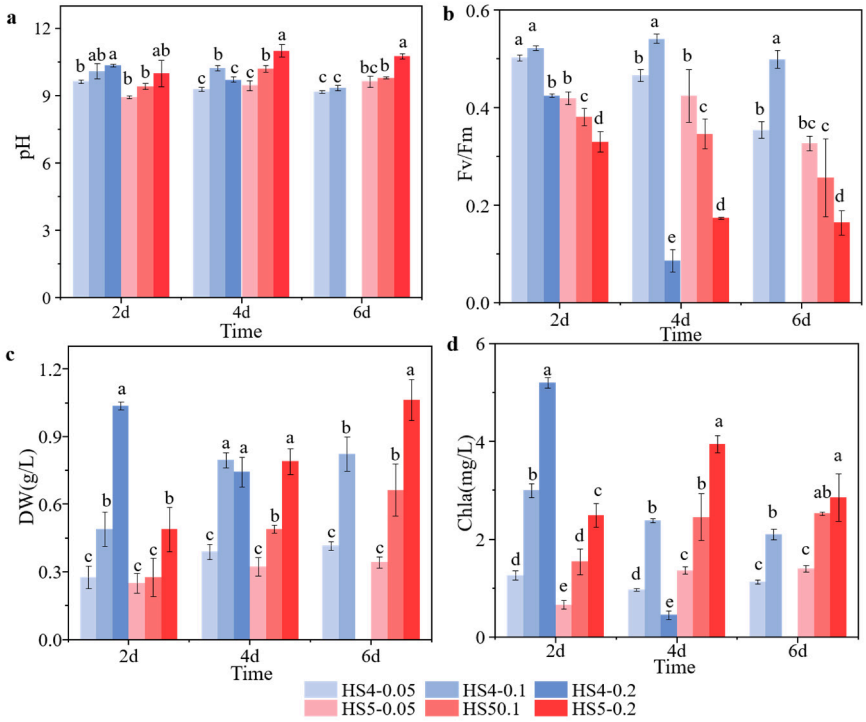


Figure 2. Changes in pH (**a**), F_v/F_m (**b**), DW (**c**) and chlorophyll (**d**) in different treatments. The 0.05, 0.1 and 0.2 represent different initial inoculum densities. Error bars represent the standard errors of the triplicate bottles. The different letters above the columns indicate a significant difference ($p < 0.05$) based on the analysis of variance.

Taken together across all measured parameters, strain HS5 at a moderate inoculum density (0.1) generally achieved a favorable balance between rapid biomass build up and sustainable growth.

3.1.3. The Impacts of Different Medium Composition Ratios

As shown in Figure S4, the microalgae in the high-inoculation treatment (0.2 g L^{-1}) exhibited more pronounced cellular damage during the late growth stage compared to the other treatments.

During cultivation, the pH increased in all treatments, ranging from 9.0 to 11.0 (Figure 3a). On day 2 and day 6, the pH rose significantly with increasing medium addition volume, with the HS5-H group showing the highest pH (10.5) and the HS5-O group the lowest (9.5). However, the HS5-Q group reached the maximum pH of 11.23 on day 4, which was significantly higher than the other two groups, while HS5-O still maintained the lowest pH. The maximum quantum yield of PSII (F_v/F_m) exhibited an overall downward trend, decreasing from around 0.41 on day 2 to roughly 0.30 on day 6. On day 2, HS5-Q obtained the highest F_v/F_m (0.41), whereas HS5-H had the lowest value (0.34). By day 4 and day 6, the F_v/F_m values became comparable across the three groups. The dry weight biomass increased significantly over time (Figure 3c). All groups yielded a low biomass (0.2–0.35 g L^{-1}) on day 2. The HS5-O group reached the highest dry weight (0.56 g L^{-1}) on day 4. At day 6, no significant difference was observed between HS5-O and HS5-Q, and both were significantly higher than HS5-H (0.55 g L^{-1}). Chlorophyll a (Chl a) concentrations showed dynamic variation. On day 2, HS5-Q and HS5-H were significantly higher than HS5-O. HS5-Q peaked at approximately 4.55 mg L^{-1} on day 4, which was markedly higher than the other two groups. No significant difference was detected on day 6, although HS5 Q still had the highest Chl a content among the three treatments. So, adding 1/4 of BG11 is more likely to promote the growth of microalgae.

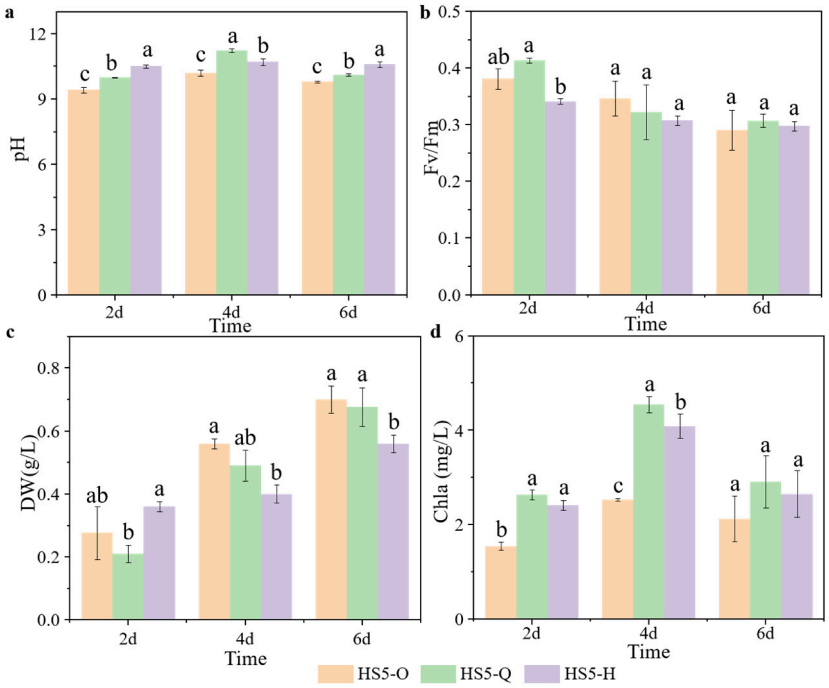


Figure 3. Changes in pH (**a**), F_v/F_m (**b**), DW (**c**) and chlorophyll (**d**) in different treatments. HS5-O, HS5-H and HS5-Q represented the XJ0 diluted with $BG11_0$ culture medium to ratios of 1:0 (HS-O), 1:1 (HS-H), 1:3 (HS-Q). Error bars represent the standard errors of the triplicate bottles. The different letters above the columns indicate a significant difference ($p < 0.05$) based on the analysis of variance.

3.1.4. The Impacts of Different Light Intensity

In this section, the effect of light intensity (25, 50 and 100 μmol m^{-2} s^{-1}) on microalgae growth was investigated. As shown in Figure S5A,B, exposure to high light intensity (100 μmol m^{-2} s^{-1}) caused visible cell damage, which was detrimental to microalgae growth.

The changes in physiological parameters under different light intensities are presented in Figure 4a–d. During cultivation, the pH increased in all treatments (Figure 4a), ranging from 9.5 to 10.9. On day 2, the pH showed no significant difference among the three groups and was positively proportional to the light intensity. On day 4 and day 6, HS5-50 and HS5-100 exhibited significantly higher pH than HS5-25, reaching approximately 10.5–10.9. The F_v/F_m declined over time across all treatments (Figure 4b), indicating progressive deterioration of photosynthetic performance. On day 2, HS5-25 and HS5-50 maintained high F_v/F_m values (0.41), whereas HS5-100 was significantly lower (0.35). At day 4 and day 6, HS5-25 retained an F_v/F_m of 0.44, while HS5-50 and HS5-100 decreased markedly to 0.220.29, suggesting that high light intensity induced photoinhibition and cellular stress responses. The dry weight biomass accumulated significantly over time and displayed a strong positive correlation with the light intensity (Figure 4c). On day 2 and day 4, the dry weight increased significantly with elevated light intensity, with HS5-100 yielding the highest values (0.48 g L^{-1} on day 2 and 0.70 g L^{-1} on day 4). By day 6, HS5-50 and HS5-100 were statistically comparable, and both were significantly higher than HS5-25 (0.45 g L^{-1}). This result implies that higher light intensity accelerates earlyphase growth, yet the differences diminish in the later phase due to nutrient limitation. The chlorophyll a (Chl a) concentration was negatively correlated with light intensity and followed first a rise and then fall trend over cultivation. No significant inter-group difference was observed on day 2. On day 4 and day 6, Chl a increased markedly in HS5-25 (4.8 mg L^{-1}), whereas HS5-50 and HS5-100 maintained relatively low levels. This demonstrates that cells acclimate

to low light conditions by elevating pigment content to enhance light-harvesting capacity. Therefore, a light intensity range of 25–50 μmol m^{-2} s^{-1} is suitable for microalgae cultivation under the studied conditions.

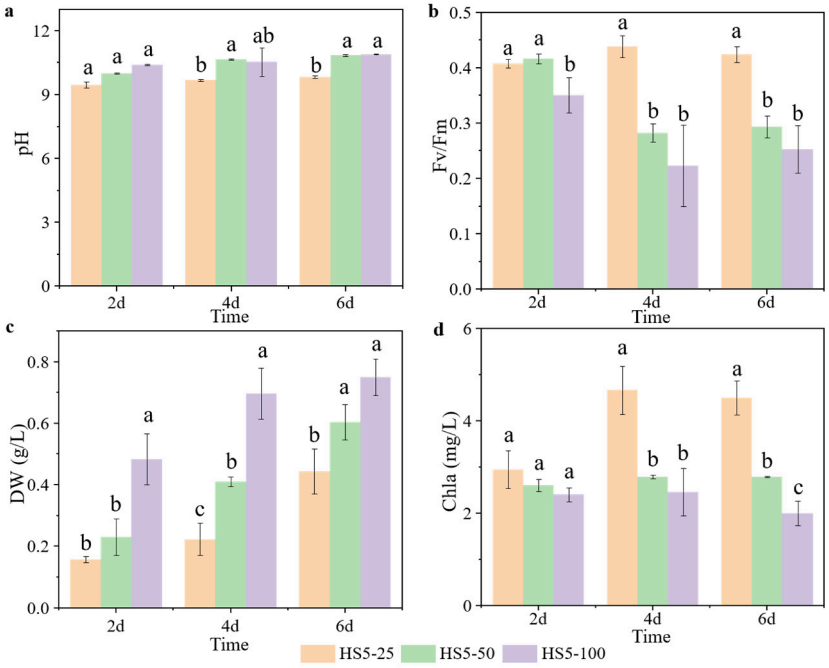


Figure 4. Changes in pH (**a**), F_v/F_m (**b**), DW (**c**) and chlorophyll (**d**) in different treatments. The 25, 50 and 100 represent alight intensity of 25, 50 and 100 μmol m^{-2} s^{-1}, respectively. Error bars represent the standard errors of the triplicate bottles. The different letters above the columns indicate a significant difference ($p < 0.05$) based on the analysis of variance.

3.2. Field Performance of Microalgae Biomass for Ecological Restoration

3.2.1. Soil Physicochemical Properties

The TN contents showed significant differences between treatments and at different time stages (Figure 5a). At the middle experiment stage, the TN contents in the three treatments showed a certain degree of increase compared to the control group. The MF treatment had the highest value at 0.695 g kg^{-1}, representing a 52.8% increase compared to the CK (0.455 g kg^{-1}). The TN in the M and F were slightly lower than that in the MF, at 0.639 g kg^{-1} and 0.662 g kg^{-1}, respectively. The MF had a further increase in TN content to 0.695 g kg^{-1}, representing a 52.8% increase compared to the CK. By the end of the experiment, the TN content in all treatments had decreased to some extent compared with those at the mid-experiment stage. In particular, the greatest decrease was observed in the CK, which reached 41.8%. The TN in the M also decreased to 0.435 g kg^{-1}, while the MF maintained a relatively high TN content (0.549 g kg^{-1}), which was 107.4% higher than that of the CK treatment. However, the AHN exhibited an accumulation trend different from that of TN (Figure 5d). At the middle experimental stage, the AHN in the M and F (15.32 mg kg^{-1} and 17.78 mg $kg^{-1,}$ respectively) were slightly higher than that in the CK (9.44 mg kg^{-1}), while in the MF treatment, the AHN increased significantly to 46.49 mg kg^{-1}, representing an increase of 392.5% compared with the CK. At the end of the experiment, the AHN in F and MF increased significantly, reaching 48.22 mg kg^{-1} and 53.08 mg kg^{-1}, respectively. Though the AHN in the M was lower than that in the F and MF, it also increased markedly to 31.45 mg kg^{-1}, which was significantly higher than that in the CK (12.75 mg kg^{-1}).

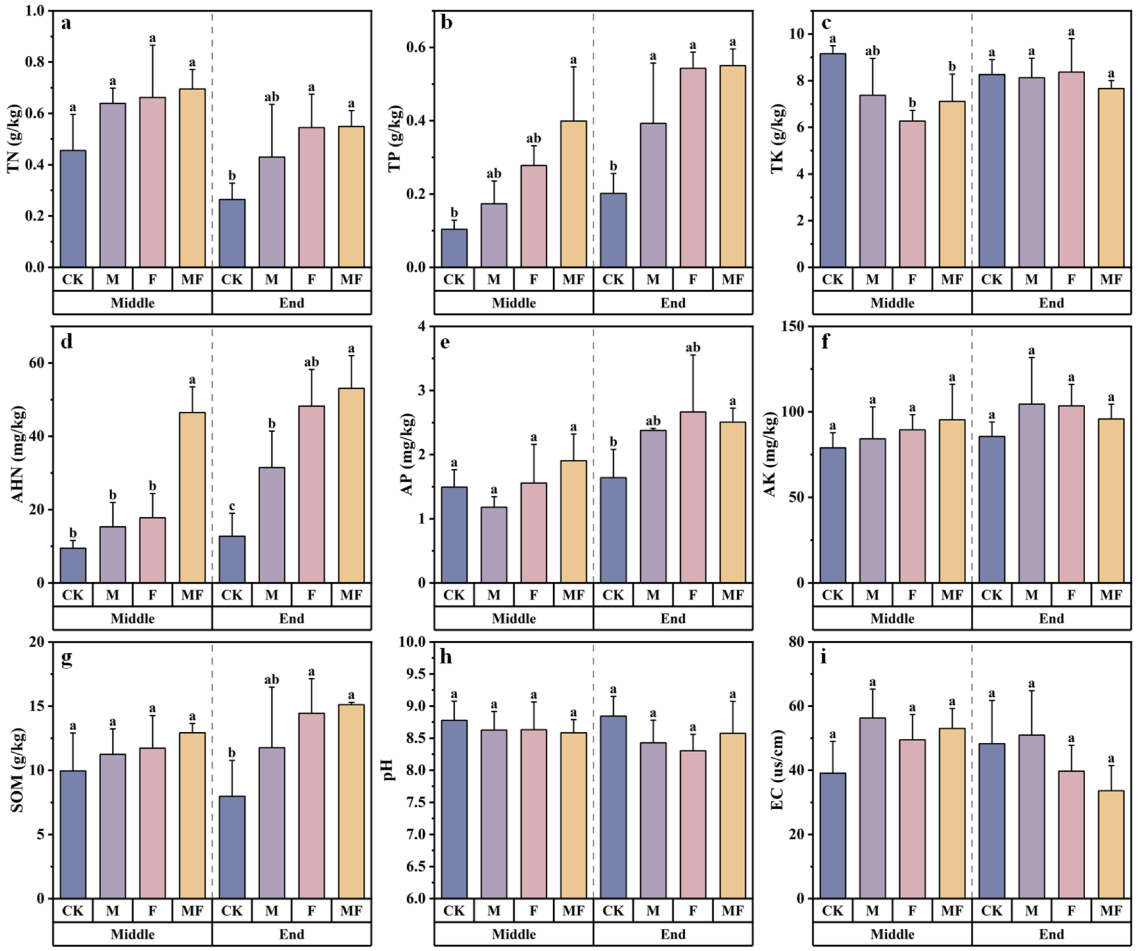


Figure 5. Soil physicochemical properties: Changes in TN (**a**), TP (**b**), TK (**c**), AHN (**d**), AP (**e**), AK (**f**), SOM (**g**), pH (**h**) and EC (**i**) at middle and end stages of the experiment. Error bars represent the standard errors of the triplicate parallel samples. The different letters above the columns indicate a significant difference ($p < 0.05$) based on the analysis of variance.

At the middle experimental stage, the individual application of microalgae or organic fertilizer increased the TP content to a certain extent, though this was not significant (Figure 5b). The TP in the M was 0.173 g kg^{-1}, which was 66.3% higher than that in the CK (0.104 g kg^{-1}). However, the combined application of cyanobacteria and organic fertilizer significantly increased the TP content to 0.399 g kg^{-1}, representing a 283.7% increase compared to the CK. The TP content continued to increase gradually over the whole experiment's duration. By the end of the experiment, the TP in all three treatments was significantly higher than that in the CK. The TP in the M was 0.393 g kg^{-1}, which was 94.6% higher than that in the CK, while the MF treatment had the highest TP, reaching 0.550g kg^{-1}, an increase of 172.68% over the CK. The AP and TP exhibited different trends (Figure 5e). At the middle experimental stage, there were no significant differences in the AP among these treatments, and the AP in the M treatment was slightly lower than that in the CK. In the end stage of the experiment, all three treatments showed varying degrees of increase compared to the CK. The AP in the M increased to 2.377 mg kg^{-1}, representing an increase of 44.9% compared with the CK, while the AP in the MF was 52.7% higher than that in the CK, slightly exceeding the increase observed in the group treated with microalgae alone.

Different from nitrogen and phosphorus, the microalgae and organic fertilizer had relatively weak effects on the soil potassium content (Figure 5c,f). The TK fluctuated during the middle experimental stage, exhibiting the highest values in the CK (9.16 g kg^{-1}). The TK in the M was slightly lower than that in the CK, while the TK in the F and MF was

significantly lower than that in the CK. By the end of the experiment, the TK in all groups tended to converge, ranging from 7.67 g kg^{-1} to 8.37 g kg^{-1}, with no significant differences among groups. The M and MF showed a slight increasing trend compared with the CK at both sampling stages. At the end of the experiment, the AK in the M (104.54 mg kg^{-1}) exhibited the highest increase, representing a 20.93% increase compared to the CK.

The SOM contents in all three treatments increased relative to the CK at the middle stage of the experiment; however, there were no differences observed between these four treatments (Figure 5g). The MF reached the highest SOM at 12.93 g kg^{-1}, while the SOM in the M and F treatments was slightly lower than the combined application treatment, with values of 11.24 g kg^{-1} and 11.73 g kg^{-1}, respectively. At the end of the experiment, the SOM in the F and MF was significantly higher than that in the CK, with the highest value in the MF at 15.12 g kg^{-1}, which was 89.5% higher than that in the CK. The SOM in the M was 11.77 g kg^{-1}, which also increased after the midpoint of the experiment and was higher than that of CK.

Figure 5h shows that the soil pH in all groups remained within the alkaline range (8.3–8.84) throughout the experimental period, without significant differences among groups. At the middle stage of the experiment, the highest pH was observed in the CK, with the other three treatments slightly lower than it (8.58–8.63). By the end of the experiment, the pH in the three treatments showed a slight downward trend. The EC also showed no significant differences among all groups during the experiment (Figure 5i). At the middle stage of the experiment, the EC increased in the M and MF, as both treatments were inoculated with microalgae. By the end of the experiment, the EC decreased in both the M and MF treatments, with the greatest decrease observed in the MF, which was the lowest value among all groups at 3.36 mS m^{-1}.

3.2.2. Plant Growth

The results of the growth parameters for sainfoin are shown in Figure 6a–d. The application of cyanobacteria and organic fertilizer significantly promoted the growth of sainfoin. In terms of fresh weight and dry weight (Figure 6a,b), the fresh weight and dry weight in the M, F, and MF treatments were significantly higher than those in the CK. Among them, the MF showed the highest performance, with the fresh weight (2.437 g) and dry weight (0.523 g) increasing by 1084.2% and 891.7%, respectively, compared with the CK. The plant height and root length are shown in Figure 6c,d; there were no significant differences among all treatments. However, the MF still had the highest plant height and root length numerically, followed by F, while the plant height in the M was lower than that in the F and MF.

The results of the growth parameters for Dahurian wildrye (*Elymus dahuricus*) are shown in Figure 6e–h. The fresh weight and dry weight of Dahurian wildrye differed significantly among treatments. The CK exhibited the lowest fresh weight and dry weight (0.078 g and 0.022 g, respectively). The M significantly increased the fresh weight and dry weight, while the F and MF further enhanced the fresh weight and dry weight, with the highest values recorded in the MF (0.671 g and 0.164 g, respectively). In terms of plant height, the CK was significantly lower than the F and MF, while plant height in the M was intermediate and showed no significant differences from the CK, F, or MF. There were no significant differences in root length among all treatments, although root length in the MF was slightly higher than with the other treatments.

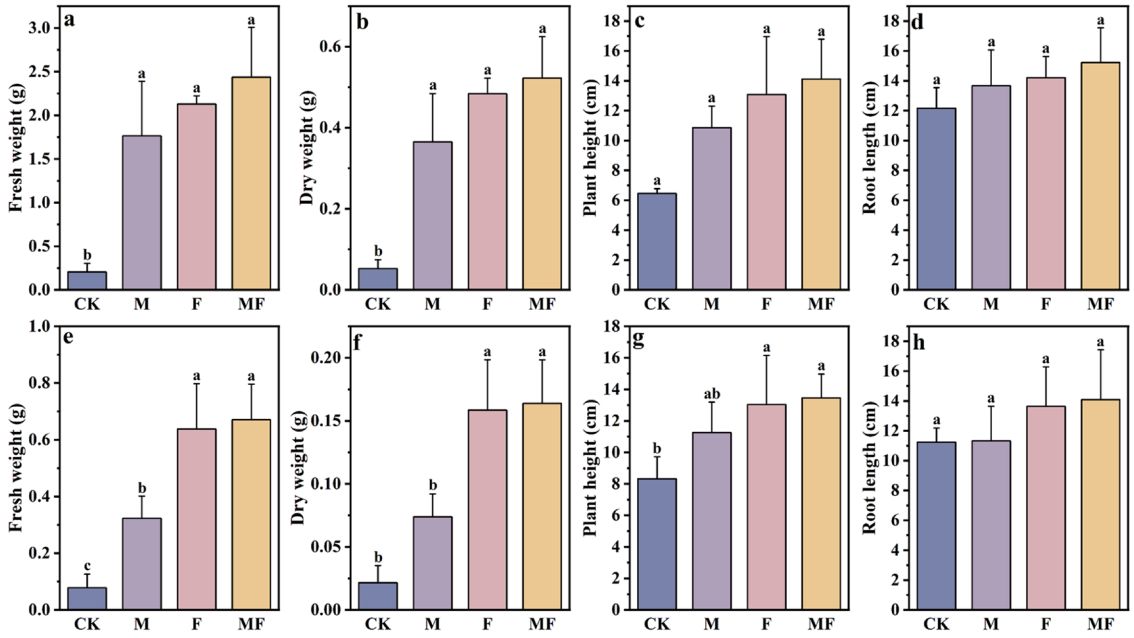


Figure 6. Plant growth changes: Sainfoin fresh weight (**a**), dry weight (**b**), plant height (**c**), and root length (**d**); Dahurian wildrye fresh weight (**e**), dry weight (**f**), plant height (**g**), and root length (**h**). Error bars represent the standard errors of the triplicate parallel samples. The different letters above the columns indicate a significant difference ($p < 0.05$) based on the analysis of variance.

3.2.3. Microbiological Diversity

Figure 7a presents the results of alpha diversity analysis. The median Shannon index was relatively high in the CK and M, with a low degree of dispersion, indicating higher species richness and community evenness in the CK and M and a relatively stable microecosystem. Compared with the CK and M, the F treatment showed a slight decrease in the median Shannon index, and its box was significantly wider. This suggests that the addition of organic fertilizer caused a sharp decline in microbial diversity in some samples, thereby increasing the within-group variation.

The principal coordinate analysis (PCoA) revealed that PC1 and PC2 explained 50.89% and 16.16% of the community variation, respectively (Figure 7b), indicating differences in the soil bacterial communities among treatments. The sample points of CK and M showed a high degree of overlap and were mainly concentrated in the negative region of PC1, whereas those of F and MF shifted toward the positive direction of PC1 and exhibited low overlap with the CK and M. The variation represented by the PC1 axis was mainly associated with changes in the soil nitrogen, phosphorus, and organic matter contents resulting from the addition of cyanobacteria and organic fertilizer. In contrast, the vertical dispersion along the PC2 axis was considerable within treatments. The pronounced dispersion of samples from the same treatment on PC2 indicates that the spatial heterogeneity of the soil microenvironment (e.g., local micro-oxic conditions, the uniformity of cyanobacterial community distribution, and the degree of degradation of organic fertilizer particles) was an important source of PC2 variation.

In Figure 7c, the Venn diagram reveals that 489 genera were shared among the four treatments, accounting for 58.28% of the total genera. The highest number of unique genera was observed in the F treatment (59), whereas the lowest was found in the CK (18).

Figure 7d shows the relative abundance at the phylum level. The dominant phyla were *Actinomycetota*, *Chloroflexota*, *Pseudomonadota*, *Bacillota*, and *Acidobacteriota*, which accounted for the vast majority of the total community; the remaining taxa, such as *Gemmatimonadota* and *Bacteroidota*, were secondary groups. Among them, *Actinomycetota* had the highest

relative abundance, ranging from 32.5% to 38.5%. The abundance of Actinomycetota was approximately the same in the CK and M, decreased in the F, and was the lowest in the MF. As the second most abundant phylum, *Chloroflexota* increased in the F and MF. Meanwhile, the abundance of *Pseudomonadota* decreased in the M and MF. The abundance of *Bacillota* showed an increasing trend in the M, F, and MF, with a significant increase in the MF. In contrast, the abundance of *Acidobacteriota* decreased in the M, F, and MF, with the most pronounced decrease observed in the MF.

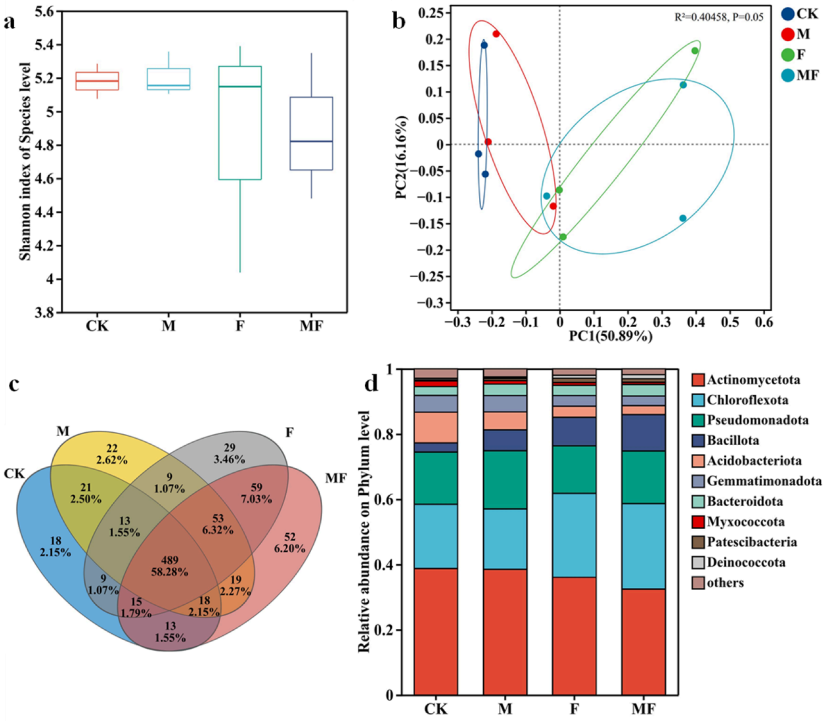


Figure 7. Shannon index of species level (**a**), principal coordinate analysis (PCoA) of microbial communities (**b**), Venn diagram of shared and unique genera (**c**), and relative abundance of bacterial phyla among different groups (**d**).

A redundancy analysis (RDA) revealed the macro-scale associations between environmental factors and sample community structure, with RDA1 and RDA2 explaining 73.61% and 6.30% of the variation, respectively (Figure 8a). The AHN, TP, SOM, AP were the main environmental factors associated with community differentiation. The F and MF samples were distributed on the right side of the RDA axis and were positively correlated with the AHN, TP, SOM, and AP, and the MF showed stronger correlations with these nutrients. The CK samples were mainly distributed on the left side of the RDA1 axis and were negatively correlated with the AHN, TP, SOM, etc., showing the greatest community differences from the F and MF treatments. For the M treatment, some sample points were close to those of CK, whereas the others were close to the F and MF treatments. The Mantel test in Figure 8b reveals the correlations between soil bacterial communities and soil physicochemical factors under different treatments. Similarly, the species-level communities in the F and MF treatments exhibited highly positive correlations with the TN, AHN, TP, AP, and SOM.

Figure 8c shows a heatmap of correlations between environmental factors and soil microbial communities at the phylum level, revealing significant differentiation in the responses of different bacterial phyla to soil nutrients. *Acidobacteriota*, *Methylomirabilota*, *Myxococcota*, *Gemmatimonadota*, and *Actinomycetota* were negatively correlated with soil nutrients, with significant negative correlations with the TP and AHN. In contrast, *Bacillota* and *Deinococcota* were highly significantly positively correlated with the TP and AHN, while

Chloroflexota, *Planctomycetota*, and *Bacteroidota* also showed positive responses to increased nutrient levels. *Cyanobacteriota* was significantly positively correlated with the SOM.

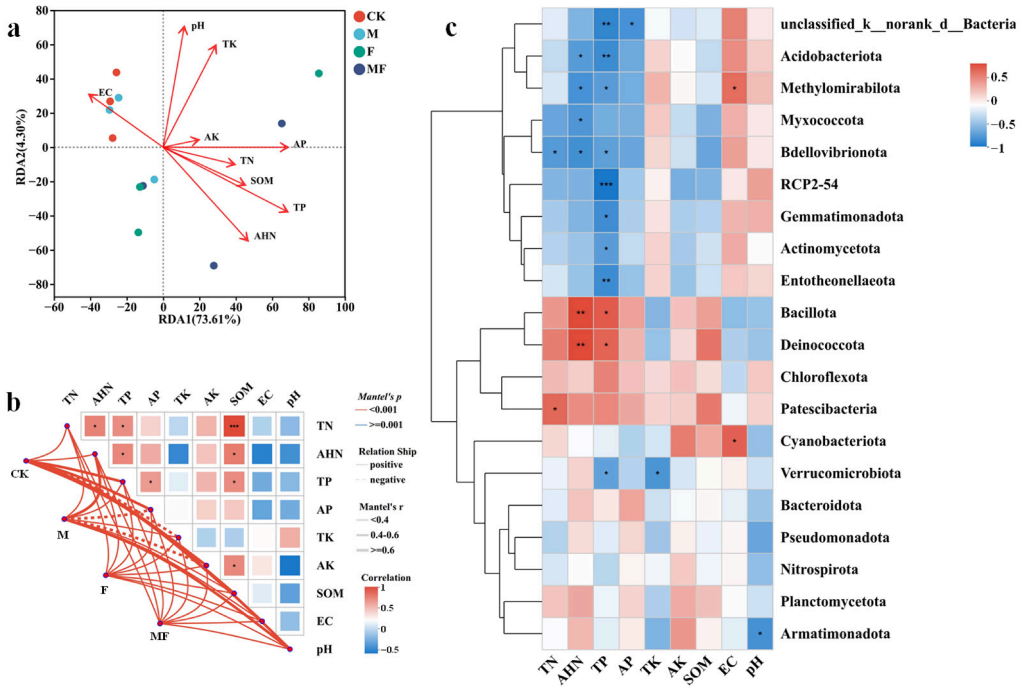


Figure 8. Redundancy analysis (RDA) of microbial communities and environmental factors (**a**), Mantel test network and correlation heatmap of environmental factors (**b**), correlation heatmap between bacterial taxa and environmental factors at phylum level (**c**). Asterisks indicate significant correlations (* $p < 0.05$, ** $p < 0.01$, *** $p < 0.001$).

4. Discussion

4.1. Different Factors Influence the Growth of Microalgae

The enhanced growth in raw water is likely attributable to its nutrient concentrations, shown in Table S1, as some of them are essential nutrients for microalgae. Carbon, nitrogen, and phosphorus in wastewater play critical roles in microalgal metabolism: carbon supplies the structural skeleton, nitrogen supports amino acid synthesis, and phosphorus is essential for ATP production and energy metabolism [56,57]. The elevated pH observed across treatments originated from a typical feature of cyanobacterial photosynthetic carbon fixation that consumes dissolved CO_2/HCO_3^- [58–60]. However, as the training period lengthened, the F_v/F_m value gradually decreased. This trend likely resulted from nitrogen and phosphorus depletion without exogenous nutrient input [61,62]. Phosphorus limitation impairs photosynthetic phosphorylation and the Calvin cycle, thereby lowering F_v/F_m. Most XJ0 cultures maintained higher F_v/F_m values than their XJ1 counterparts, which was also linked to nutrient limitation [61]. In the late phase, the DW and Chl a were decoupled: the DW kept increasing while the Chl a plateaued or decreased. Such divergence suggests that later stage biomass gain was partially caused by extracellular polymeric substance (EPS) accumulation and polysaccharide-driven adsorption of suspended solids in raw mine water. Cyanobacteria secrete EPS as a primary protective barrier under nutrient and metal stress [63,64]; enhanced EPS synthesis has been documented in salt-tolerant nitrogen-fixing cyanobacteria under salinity and metal stress [65].

The initial biomass concentration of microalgae strongly affects lag-phase duration, specific growth rate, and biomass accumulation dynamics [66]. The highest density groups (HS4-0.2, HS5-0.2) consistently maintained maximum pH, suggesting that an elevated initial

cell density accelerates photosynthetic activity and nutrient consumption [58]. However, the F_v/F_m ranged from 0.15 to 0.55 and sharp F_v/F_m drops occurred on days 46, especially under 0.2 inoculum density, reflecting nutrient depletion and impaired photosynthetic performance [67,68]. For HS4-0.2, biomass decreased markedly after day 2. This may be attributable to an excessively high inoculum concentration, which consumed excessive nutrients from the medium during early growth, causing extensive algal cell death and decomposition (Figure S3) and thus leading to a pronounced decline in biomass after day 2. This phenomenon indicates that although high initial cell density confers an early-phase growth advantage, it aggravates self-shading and impedes light penetration, thereby reducing photosynthetic efficiency and specific growth rate [66,69]. The similar decoupling of dry weight (DW) and Chl a in later cultivation phases implies that under nutrient limited or high density conditions, carbon flux may shift away from pigment synthesis toward the production of storage compounds such as polysaccharides or extracellular polymeric substances, reflecting a physiological reprogramming of algal cells [70,71].

Light intensity acted as a critical modulator shaping the growth and photosynthetic physiology of microalgae [72]. In this study, we found that although high irradiance (100 μmol m^{-2} s^{-1}) promoted early phase biomass accumulation, it triggered obvious photoinhibition, as reflected by the sharp drop in F_v/F_m at the later stage [73]. Under high light stress, cells consume substantial metabolic resources for PSII-repair machinery, which partially offsets the growth advantages [74].

This study also investigated the growth and photosynthetic responses of the diazotrophic cyanobacterium HS5 cultivated in XJ0 (HS5-O), XJ0 diluted with BG11 culture medium to ratios of 1:3 (HS5-Q), and XJ0 diluted with BG11 culture medium to ratios of 1:1 (HS5-H). Raw mine water contained trace-level phosphorus (TP < 0.01 mg L^{-1}) as well as metals such as As and Se. Although the mine water favoured microalgal growth in the early phase, it exerted certain stress effects over long-term cultivation [75]. Overall, HS5-Q exhibited higher F_v/F_m and chl a concentrations than HS5-O and HS5-H, demonstrating that moderate nutrient supplementation with a small amount of BG11 could sustain favourable photosynthetic performance in the mine-water matrix. By comparison, supplementation with more BG11 (HS5-H) failed to further improve photosynthetic capacity and triggered more severe cellular damage at the later growth stage (Figure S4). Raw mine water is rich in total soluble solids, SO_4^{2-} and heavy metals [76]. When combined with nutrients from the added medium, even increased macronutrient supply imposes metabolic pressure on microalgae, impairs cellular integrity, and diverts carbon flux away from growth towards stress-defense metabolism [70].

4.2. Effects of Microalgal Biomass on Soil Physicochemical Properties, Plant Growth, and Soil Microorganisms

The soil organic matter (SOM) is a core indicator for evaluating soil fertility, and changes in its content can reflect the accumulation and mineralization dynamics of the soil carbon stock following exogenous organic matter [77,78]. The application of cyanobacteria alone was able to increase the SOM content. The cyanobacterial biomass itself contained large amounts of intracellular organic carbon; after inoculation in the soil, part of it was rapidly decomposed and released as organic matter, supplementing the SOM in the short term [79–81]. However, due to the much lower application amount compared to organic fertilizer, the cyanobacteria had a limited effect on increasing the soil organic matter. In contrast, the combined application of cyanobacteria and organic fertilizer further increased the SOM content compared with cyanobacteria or organic fertilizer alone. This is attributed to the combined effects of cyanobacteria and organic fertilizer. The organic fertilizer provided humus as a carbon source, while the cyanobacteria supplied an active carbon source

for soil microorganisms, stimulating microbial proliferation [82,83]. Therefore, at the late stage of the experiment, the SOM content in the M treatment remained comparable to that at the mid-experiment stage due to the limited amount of cyanobacteria inoculated. In the MF treatment, however, recalcitrant components in the organic fertilizer were decomposed by microorganisms to provide organic matter to the soil [84]. Meanwhile, extracellular polysaccharides (EPSs) secreted by the cyanobacteria bound organic fertilizer particles with fine soil particles, forming stable aggregates that physically protected the organic carbon from rapid mineralization [85–87].

There were no significant changes in the pH; this may have been because the experiment lasted only 90 days and the relatively short experimental period did not exert a significant effect on the pH. In the middle stage of the experiment, the EC of the M, F, and MF groups increased, possibly because the nutrients released from the microalgal cells and organic fertilizer into the soil increased the soil EC. However, in the late stage of the experiment, the EC of the F and MF groups decreased markedly. This may have been because the addition of organic fertilizer increased the soil porosity and leaching during irrigation, causing ions to migrate to deeper soil layers, while the extracellular polysaccharides produced by the cyanobacteria acted as binders that reduced soil porosity and thereby decreased the leaching losses of soil components.

Soil nitrogen (N) and phosphorus (P), as core nutrient elements, are the primary limiting nutrients affecting plant growth [88,89]. At the middle experimental stage, microalgae application increased the soil N and P contents. Cyanobacterial biomass is rich in components such as proteins, phospholipids, and polyphosphates [90,91]. After application to soil, cyanobacteria can fix nitrogen from the air and convert it into biomass, and some cyanobacterial cells are rapidly decomposed by microorganisms, releasing ammonium nitrogen and bound phosphorus through ammonification, thereby increasing the soil total nitrogen (TN), available nitrogen (AN), total phosphorus (TP), and available phosphorus (AP) contents [80,92]. However, on the one hand, the N and P contents within microalgae are limited; on the other hand, the ammonium nitrogen produced by mineralization is at risk of volatilization or leaching, and the released phosphorus can chemically bind with calcium, iron, and aluminum ions in the soil [93–95]. In the combined application of microalgae and organic fertilizer (MF treatment), the soil N content was higher than that under microalgae or organic fertilizer alone, indicating a complementary and combined effect between the two [96,97]. The organic fertilizer continuously supplied organic N and P, while the cyanobacteria stimulated microbial proliferation, promoting N and P mineralization and the activation of the inherent insoluble phosphorus in the soil, thereby achieving the simultaneous accumulation of N and P [98,99]. At the late stage of the experiment, the recalcitrant organic matter in the soil was continuously decomposed and mineralized, and the AHN content continued to increase [100,101]. However, the TN content decreased in all treatments. First, the soil pH ranged from 8.3 to 8.8, indicating an alkaline environment in which NH_4^+ readily combined with OH^- to form free ammonia, leading to ammonia volatilization [102]. Simultaneously, nitrification occurred in the soil, in which NH_4^+ was converted to NO_3^-, and NO_3^- was reduced to N_2 by denitrifying bacteria and escaped [101]. In the CK group, plant growth consumed soil nitrogen, while ammonia volatilization and leaching further reduced the soil nitrogen content. Moreover, unlike the M, F, and MF groups, the CK group received no additional nitrogen input; therefore, the nitrogen content in the CK group declined markedly in the late stage of the experiment. Although the extracellular polymeric substances (EPSs) produced by microalgae contain acidic functional groups that can release protons and lower the pH of alkaline soils, the short-term treatment did not significantly reduce soil pH. The potential reduction in soil pH following long-term cyanobacterial application needs to be considered, as lowering

the soil pH can shift the NH_4^+/NH_3 equilibrium and reduce ammonia volatilization. In addition, drip fertigation is the single most effective management improvement measure; it has been reported that, in alkaline soils, cumulative NH_3 emissions under drip fertigation are 55.93% lower than under furrow irrigation. These strategies are proposed based on existing evidence; however, their effectiveness under the specific cold and arid irrigated conditions of this experiment remains to be verified [103,104]. In contrast, the phosphorus content increased because the organic fertilizer continuously input organic phosphorus, which slowly decomposed to release phosphorus [105]. Moreover, the organic acids and phosphatases secreted by cyanobacterial metabolism effectively promoted the activation and release of sparingly soluble phosphorus by competing for adsorption sites on soil colloids and chelating metal ions (e.g., Ca^{2+} and Fe^{3+}), thereby increasing both the TP and AP [106,107]. Compared with nitrogen and phosphorus, the soil potassium pool was larger and had a strong buffering capacity for potassium; therefore, the effects of the treatments on soil potassium were less pronounced than those on nitrogen and phosphorus. In the F and MF, plant growth, particularly that of Dahurian wildrye, was considerably greater than that in the CK group, and this growth consumed soil potassium.

The growth trends of sainfoin and Dahurian wildrye were generally consistent with the variation trends of soil organic matter and soil nutrients. The growth parameters of both species were highest in the MF treatment, lower in the M treatment than in the F and MF treatments, and lowest in the CK. However, sainfoin and Dahurian wildrye exhibited different growth responses to cyanobacteria and organic fertilizer. There was no significant difference in the growth-promoting effects on sainfoin between the application of cyanobacteria and organic fertilizer alone, whereas cyanobacteria alone only slightly increased the biomass of Dahurian wildrye, and the growth promotion of Dahurian wildrye was more dependent on organic fertilizer. This may be attributed to the synergistic effect between the inherent rhizobial nitrogen fixation of sainfoin as a legume and exogenous nutrient supply [45,46]. Sainfoin, through rhizobia, can fix atmospheric nitrogen, and its dependence on soil nitrogen supply is lower than that of grasses [108]. In addition, the cyanobacteria can supplement nitrogen sources through biological nitrogen fixation by cyanobacteria itself, while cyanobacterial extracellular polysaccharides can improve soil aggregate structure and enhance water- and fertilizer-retention capacity [20]. In contrast, Dahurian wildrye, as a gramineous forage, has no biological nitrogen fixation capacity, and its growth depends on available soil nutrients. Organic fertilizer continuously supplies available nitrogen and phosphorus through organic matter mineralization, which is more sufficient than the nitrogen and phosphorus supplied by cyanobacteria. It should be noted that in arid/semi-arid mining areas, the amount of irrigation water is a key factor in soil restoration. In this experiment, water usage was significantly lower than that required for large-scale grassland restoration in arid/semi-arid mining areas 1.33 L m^{-2} d^{-1}. Although this experiment lasted 90 days and focused on revegetation and soil-surface stabilization, mine water may contain potentially toxic metals that can be accumulated by microalgae and plants, which form the base of primary food chains. Such accumulation could pose toxicological risks to primary consumers and, where restored grasslands are grazed, may create a pathway for contaminants to enter livestock food chains [109,110]. In this study, metal accumulation in algal or plant biomass, contaminant bioavailability, and food chain transfer were not measured; therefore, the toxicological risk of the present system remains to be quantified. Future studies should combine tissue metal analysis, bioaccessibility assays, and food chain transfer assessments before the system is applied at sites where mining-derived contaminants may enter agricultural or pastoral food chains.

As a legume, sainfoin influences soil microbial populations through rhizobia; the different treatments also altered the soil microbial communities. At the phylum level, the soil

bacteria in the four treatments were dominated by *Actinomycetota*, *Chloroflexota*, *Pseudomonadota*, *Bacillota*, and *Acidobacteriota*, but the community composition differed significantly among treatments. Compared with the CK group, the relative abundance of the Actinobacteria phylum in the M group decreased slightly, while that of the *Chloroflexota* and *Bacillota* phyla increased. In the MF treatment, the abundance of *Actinomycetota* further decreased, the relative abundances of *Chloroflexota* and *Bacillota* reached the highest levels among all treatments, and the abundance of *Acidobacteriota* continued to decline. These results, combined with the RDA, Mantel test, and the heatmap of correlations between environmental factors and microbial communities, revealed that the M treatment initially altered the soil nutrient environment through the biological characteristics of cyanobacteria themselves, as the inoculation of cyanobacteria promotes the growth of copiotrophic bacteria [79]. The MF treatment amplified the nutrient supply effect through the combined coupling of cyanobacteria and organic fertilizer that formed a unique soil microenvironment, and drove directed succession in the bacterial community. The abundances of *Acidobacteriota*, which prefer oligotrophic environments, decreased significantly [111,112]. In contrast, *Bacillota*, *Bacteroidota*, and other copiotrophic taxa with efficient organic matter degradation capacity were significantly enriched [113,114]. Bacteroidota and Bacillota, as copiotrophic taxa, respond rapidly to increases in soil nutrient and organic matter levels [113,115]. They grow and multiply rapidly by utilizing easily degradable organic matter and participate in nutrient cycling; the organic matter they decompose further increases soil nutrient levels. Both *Actinomycetota* and *Chloroflexota* possess the ability to degrade complex soil organic matter. However, in the F and MF treatments, the abundance of *Actinomycetota* decreased while that of *Chloroflexota* increased. There is no definitive conclusion regarding whether *Actinomycetota* are eutrophic or oligotrophic conditions, but some studies have shown that the abundance of *Actinomycetota* in soil decreases after the addition of organic fertilizer [112,114]. Furthermore, after entering soil, organic fertilizer enhances soil microbial activity and consumes large amounts of oxygen, creating local hypoxic or anoxic zones in the soil [116]. Many members of *Chloroflexota* are facultative anaerobes and can adapt to this environment, thereby competing ecologically with *Actinomycetota*, since the majority of *Actinomycetota* are aerobic bacteria [117–119]. *Actinomycetota* possess a strong capacity to secrete extracellular enzymes (e.g., cellulases and chitinases) and are adept at the aerobic degradation of complex polymers. However, under anoxic conditions, the synthesis and activity of their extracellular enzymes decline substantially, preventing them from efficiently acquiring carbon sources. In contrast, although *Chloroflexota* generally have a weaker capacity for the direct degradation of complex polymers, many taxa are adept at utilizing simpler fermentation intermediates, such as sugars and organic acids. This may also explain why the abundance of *Actinomycetota* decreased while that of *Chloroflexota* increased. However, in the M treatment, cyanobacteria produced oxygen through photosynthesis in the soil, resulting in fewer hypoxic or anoxic zones, and the abundance of *Chloroflexota* was significantly lower than that in the F and MF treatments. The RDA results showed that the MF samples were independently distributed in the ordination space. The Mantel test demonstrated that the bacterial community in the MF treatment was significantly associated with soil environmental factors, such as TN, AHN, SOM, and TP. These indicate that the filtering effect of physicochemical factors on the bacterial community is significantly enhanced when cyanobacteria and organic fertilizer are applied together.

This study demonstrates the technical feasibility of cultivating microalgae with mine water and applying the resulting biomass to the mining area's ecological restoration under controlled laboratory conditions. However, caution is required when extrapolating these findings to field scale. First, the laboratory trials were conducted under relatively stable physicochemical conditions, whereas fluctuations in the quality of actual mine water, to-

gether with variations in light and temperature, precipitation, and biological contamination by indigenous microorganisms and grazers during outdoor cultivation, may all reduce biomass productivity and process stability. Second, the efficacy of the active microalgal fertilizer depends on the successful colonization of the target soil by microalgae; this colonization is co-regulated by the soil conditions, climatic factors, and the indigenous soil microbial community, and thus requires optimization and validation through multi-season field trials. Finally, the economic feasibility and carbon/water footprints of this technological route should be comprehensively assessed within the frameworks of techno-economic analysis and life-cycle assessment, in order to clarify its applicable conditions in different mine site scenarios and identify viable engineering scale-up pathways, thereby laying a foundation for future large-scale application.

5. Conclusions

In summary, when untreated mine water was supplemented with partial BG11 medium, under a light intensity of 25–50 μmol m^{-2} s^{-1} and an initial inoculation density of 0.1 g L^{-1}, microalgae exhibited higher photosynthetic activity, biomass accumulation, and chlorophyll a content, and was also the best-performing condition for culturing the selected strain HS5. In the soil restoration experiments in mining areas, the combined application of cyanobacteria and organic fertilizer shows the highest soil demonstrates the highest soil organic matter and nutrient contents, as well as the strongest plant growth-promoting effect. Compared with the CK, the TN and TP increased by 107.4% and 172.68%, respectively, and the SOM increased by 89.5%. The MF treatment drove the remodeling of the microbial community by significantly increasing the soil AHN, TP, SOM, and AP contents. This was specifically reflected in the significant enrichment of beneficial functional taxa, such as *Bacillota* and *Bacteroidota*, and a reduction in the abundance of the oligotrophic *Acidobacteriota*; among these factors, the SOM was the core driving factor. This study demonstrates the feasibility of using mine water as an alternative water source for microalgae cultivation and of utilizing the cultivated microalgae biomass for soil restoration in mining areas. This approach not only reduces cultivation costs but also addresses the shortage of clean water in the local area, thereby providing a theoretical basis for comprehensive ecological restoration of mining areas in northwestern China.

Supplementary Materials: The following supporting information can be downloaded at: https://www.mdpi.com/article/10.3390/w18212790/s1, Figure S1: A diagram of experimental site division; Figure S2: Changes in the experimental pictures (A) and microscopic images (B) for different treatments at 0d, 2d, 4d and 6d. HS1-5 represent different microalgae, XJ0 is raw water and XJ1 is flocculated water; Figure S3: Changes in the experimental pictures (A) and microscopic images (B) for different treatments at 0d, 2d, 4d and 6d. The numbers 0.05, 0.1 and 0.2 represent different initial inoculum densities; Figure S4: Changes in the experimental pictures (A) and microscopic images (B) at 0d, 2d, 4d and 6d. HS5-O, HS5-Q and HS5-H represent medium addition ratios of 1:0, 1:1, and 1:3, respectively; Figure S5: Changes in the experimental pictures (A) and microscopic images (B) at 0d, 2d, 4d and 6d. HS5-25, HS5-50 and HS5-100 represent alight intensity of 25, 50 and 100 μmol m^{-2} s^{-1} inoculating HS5, respectively; Table S1: The physiochemical properties of the mine water; Table S2: The culture parameters of different operating conditions.

Author Contributions: P.Y.: Writing—original draft, Conceptualization, Methodology, Data Curation, and Validation; B.H.: Methodology, Data Curation, and Visualization; J.Z.: Methodology and Investigation; X.Z.: Formal analysis and Investigation; Z.X.: Formal analysis and Investigation; T.T.: Methodology, Investigation, and Funding acquisition; R.Z.: Investigation and Formal analysis; D.X.: Data Curation and Validation; Y.H.: Writing—review and editing, Conceptualization, and Funding acquisition; K.L.: Writing—review and editing, Conceptualization, Project administration, and Supervision. All authors have read and agreed to the published version of the manuscript.

Funding: This work was supported by Shanghai Agricultural Science and Technology Innovation Projects (A2024010).

Data Availability Statement: The data presented in this study are available on request from the corresponding author due to privacy.

Conflicts of Interest: Authors Peng Yu, Xufan Zheng, Zhikun Xin, Rui Zhao, Dong Xu were employed by the company ChnEnergy New Energy Technology Research Institute Co., Ltd. The remaining authors declare that the research was conducted in the absence of any commercial or financial relationships that could be construed as potential conflicts of interest.

References

1. Han, T.; Li, Q.Y.; Hai, Y.; Yang, Y.Z.; Wen, Z.; Li, R.N.; Zheng, H. Response of ecosystem services and environmental dynamics in large open-pit coal mines: A case study in semi-arid areas. *Glob. Ecol. Conserv.* **2024**, *51*, e02891. [CrossRef]
2. Yan, X.X.; Li, J.; Shao, Y.; Ma, T.Y.; Zhang, R.; Su, Y.T. Assessing open-pit mining impacts on semi-arid grassland: A framework for boundary and intensity quantification. *J. Clean. Prod.* **2024**, *475*, 143464. [CrossRef]
3. Misebo, A.M.; Woś, B.; Gruba, P.; Pietrzykowski, M. Reclamation and vegetation effects on labile and stable soil organic carbon fractions in a spoil heap of coal mining waste. *Pedosphere* **2026**, *36*, 738–748. [CrossRef]
4. Yao, Y.; Dai, Q.; Gao, R.; Yi, X.; Wang, Y.; Hu, Z. Characteristics and factors influencing soil organic carbon composition by vegetation type in spoil heaps. *Front. Plant Sci.* **2023**, *14*, 1240217. [CrossRef] [PubMed]
5. Zhou, S.Y.; Duan, Y.F.; Zhang, Y.X.; Guo, J.J. Vegetation dynamics of coal mining city in an arid desert region of Northwest China from 2000 to 2019. *J. Arid Land* **2021**, *13*, 534–547. [CrossRef]
6. Liu, H.L.; Wang, H.F.; Sun, J.Q.; Yang, T.H.; Mo, Z.X.; Huang, H.; Pan, Y.B. High-altitude open-pit coal mining has changed the sulfur cycle and ecological network of plant rhizosphere microorganisms. *Ecol. Evol.* **2025**, *15*, e71183. [CrossRef] [PubMed]
7. Zhao, W.; Huang, J.W.; Wang, K.; Hu, P.F.; Huang, Y.; Li, C.X.; Zhu, Y.X.; Fan, L.; Zhao, L.J. How to restore ecology and reduce carbon emissions in abandoned mines in a safe and environmentally friendly way? *Process Saf. Environ. Prot.* **2025**, *194*, 1558–1571. [CrossRef]
8. Rodríguez-Espinosa, T.; Pérez-Gimeno, A.; Almendro-Candel, M.B.; Navarro-Pedreño, J.; García-Fernández, G. Technosols for mine restoration: Overcoming challenges and maximising benefit. *Appl. Sci.* **2025**, *15*, 11664. [CrossRef]
9. Aparicio, J.D.; Raimondo, E.E.; Saez, J.M.; Costa-Gutierrez, S.B.; Álvarez, A.; Benimeli, C.S.; Polti, M.A. The current approach to soil remediation: A review of physicochemical and biological technologies, and the potential of their strategic combination. *J. Environ. Chem. Eng.* **2022**, *10*, 107141. [CrossRef]
10. Feng, S.; Li, Z.; Zhang, C.; Qi, R.; Yang, L. Ecological restoration in high-altitude mining areas: Evaluation soil reconstruction and vegetation recovery in the Jiangcang coal mining area on the Qinghai-Tibet Plateau. *Front. Environ. Sci.* **2025**, *12*, 1538243. [CrossRef]
11. Igwe, O.; Ayogu, C.N.; Maduka, R.I.; Ayogu, N.O.; Ugwoke, T.A. Slope failures and safety index assessment of waste rock dumps in Nigeria's major mines. *Nat. Hazards* **2023**, *115*, 1331–1370. [CrossRef]
12. Song, W.; Xu, R.; Li, X.; Min, X.; Zhang, J.; Zhang, H.; Hu, X.; Li, J. Soil reconstruction and heavy metal pollution risk in reclaimed cultivated land with coal gangue filling in mining areas. *Catena* **2023**, *228*, 107147. [CrossRef]
13. Rodriguez-Franco, C.; Page-Dumroese, D.S. Woody biochar potential for abandoned mine land restoration in the US: A review. *Biochar* **2021**, *3*, 7–22. [CrossRef]
14. Lázaro-González, A.; Andivia, E.; Hampe, A.; Hasegawa, S.; Marzano, R.; Santos, A.M.; Castro, J.; Leverkus, A.B. Revegetation through seeding or planting: A worldwide systematic map. *J. Environ. Manag.* **2023**, *337*, 117713. [CrossRef] [PubMed]
15. Neuenkamp, L.; Prober, S.M.; Price, J.N.; Zobel, M.; Standish, R.J. Benefits of mycorrhizal inoculation to ecological restoration depend on plant functional type, restoration context and time. *Fungal Ecol.* **2019**, *40*, 140–149. [CrossRef]
16. Rawat, V.S.; Kaur, J.; Bhagwat, S.; Pandit, M.A.; Rawat, C.D. Deploying microbes as drivers and indicators in ecological restoration. *Restor. Ecol.* **2023**, *31*, e13688. [CrossRef]
17. Xu, H.L.; Qiao, X.; Gao, G.K.; Dou, H.T.; Waheed, A.; Aili, A. Advances in ecological restoration of mining–impacted landscapes: Techniques, case studies, and key challenges. *Environ. Res.* **2026**, *290*, 123485. [CrossRef] [PubMed]
18. Ramakrishnan, B.; Maddela, N.R.; Venkateswarlu, K.; Megharaj, M. Potential of microalgae and cyanobacteria to improve soil health and agricultural productivity: A critical view. *Environ. Sci. Adv.* **2023**, *2*, 586–611. [CrossRef]
19. Song, X.; Bo, Y.; Feng, Y.; Tan, Y.; Zhou, C.; Yan, X.; Ruan, R.; Xu, Q.; Cheng, P. Potential applications for multifunctional microalgae in soil improvement. *Front. Environ. Sci.* **2022**, *10*, 1035332. [CrossRef]

20. Nawaz, T.; Joshi, N.; Nelson, D.; Saud, S.; Abdelsalam, N.R.; Abdelhamid, M.M.A.; Jaremko, M.; Rahman, T.U.; Fahad, S. Harnessing the potential of nitrogen–fixing cyanobacteria: A rich bio–resource for sustainable soil fertility and enhanced crop productivity. *Environ. Technol. Innov.* **2024**, *36*, 103886. [CrossRef]
21. Yadav, P.; Singh, R.P.; Rana, S.; Joshi, D.; Kumar, D.; Bhardwaj, N.; Gupta, R.K.; Kumar, A. Mechanisms of stress tolerance in cyanobacteria under extreme conditions. *Stresses* **2022**, *2*, 531–549. [CrossRef]
22. Hu, W.B.; Wang, X.M.; Xu, Y.F.; Wang, X.; Guo, Z.Y.; Pan, X.Z.; Dai, S.X.; Luo, Y.M.; Teng, Y. Biological nitrogen fixation and the role of soil diazotroph niche breadth in representative terrestrial ecosystems. *Soil Biol. Biochem.* **2024**, *189*, 109261. [CrossRef]
23. Wu, H.W.; Cui, H.L.; Fu, C.X.; Li, R.; Qi, F.Y.; Liu, Z.L.; Yang, G.; Xiao, K.Q.; Qiao, M. Unveiling the crucial role of soil microorganisms in carbon cycling: A review. *Sci. Total Environ.* **2024**, *909*, 168627. [CrossRef] [PubMed]
24. Afkairin, A.; Ippolito, J.A.; Stromberger, M.; Davis, J.G. Solubilization of organic phosphorus sources by cyanobacteria and a commercially available bacterial consortium. *Appl. Soil Ecol.* **2021**, *162*, 103900. [CrossRef]
25. Yandigeri, M.S.; Yadav, A.K.; Srinivasan, R.; Kashyap, S.; Pabbi, S. Studies on mineral phosphate solubilization by cyanobacteria Westiellopsis and Anabaena. *Microbiology* **2011**, *80*, 558–565. [CrossRef]
26. Simon, V.; Lorenzato, J.; Mulinari, J.; Bortoluzzi, E.C.; Rempel, A.; Nazari, M.T.; Colla, L.M. Phosphorus and potassium mobilization from rock-derived mineral sources using bacteria and microalgae: A review. *Microorganisms* **2026**, *14*, 1761. [CrossRef] [PubMed]
27. Nawaz, T.; Saud, S.; Gu, L.P.; Khan, I.; Fahad, S.; Zhou, R.B. Cyanobacteria: Harnessing the power of microorganisms for plant growth promotion, stress alleviation, and phytoremediation in the era of sustainable agriculture. *Plant Stress* **2024**, *11*, 100399. [CrossRef]
28. Tripathi, R.; Singh, V.K.; Rana, P.; Jha, S.; Singh, A.P.; Rana, P.; Sinha, R.P. Metabolic adaptations of cyanobacteria to environmental stress: Mechanisms and biotechnological potentials. *Phyton-Int. J. Exp. Bot.* **2025**, *94*, 3371–3399. [CrossRef]
29. Maurya, N.; Sharma, A.; Dubey, J.; Sundaram, S. Role of cyanobacterial exopolysaccharide in soil fertility: Composition, mechanism and application. *Curr. Microbiol.* **2026**, *83*, 390. [CrossRef] [PubMed]
30. Mager, D.M.; Thomas, A.D. Extracellular polysaccharides from cyanobacterial soil crusts: A review of their role in dryland soil processes. *J. Arid Environ.* **2011**, *75*, 91–97. [CrossRef]
31. Chen, Z.X.; Li, T.; He, X.Y.; Yang, H.; Huang, F.; Cao, J.H.; Wang, P.; Wang, G.H. Construction of composite biological soil crusts accelerates early-stage soil restoration in karst rocky desertification areas. *Environ. Earth Sci.* **2026**, *85*, 400. [CrossRef]
32. Aye, N.T.T.; Yizhaq, H.; Zaady, E.; Zubkov, M.V.; Kamennaya, N.A. Polysaccharide-rich cyanomass showed potential for long-term stabilization and ecological restoration of compression-degraded soils in arid drylands. *J. Environ. Manag.* **2026**, *414*, 130471. [CrossRef] [PubMed]
33. Chan, S.S.; Lee, S.Y.; Ling, T.C.; Chae, K.J.; Srinuanpan, S.; Khoo, K.S. Unlocking the potential of food waste as a nutrient goldmine for microalgae cultivation: A review. *J. Clean. Prod.* **2025**, *492*, 144753. [CrossRef]
34. Sarker, N.K.; Kaparaju, P. A critical review on the status and progress of microalgae cultivation in outdoor photobioreactors conducted over 35 years (1986–2021). *Energies* **2023**, *16*, 3105. [CrossRef]
35. Hu, X.; Zhang, Q. Mine water treatment, resource utilization and prospects in coal mining areas of western China. *Mine Water Environ.* **2024**, *43*, 210–230. [CrossRef]
36. Dong, S.; Xu, B.; Yin, S.; Han, Y.; Zhang, X.; Dai, Z. Water resources utilization and protection in the coal mining area of northern China. *Sci. Rep.* **2019**, *9*, 1214. [CrossRef] [PubMed]
37. Matebese, F.; Mosai, A.K.; Tutu, H.; Tshentu, Z.R. Mining wastewater treatment technologies and resource recovery techniques: A review. *Heliyon* **2024**, *10*, e24730. [CrossRef] [PubMed]
38. Wang, Y.J.; Peng, J.M.; Mao, Y.Y.; Liu, Z.S.; Zhao, G.H.; Zhang, F.G. Prediction of the potentially suitable areas of *Elymus dahuricus* Turcz in China under climate change based on Maxent. *Sci. Rep.* **2025**, *15*, 17959. [CrossRef] [PubMed]
39. Li, Y.J.; Zhao, Y.; Song, Z.F.; Deng, Y.N.; Wang, H.; Xu, L.Y.; Cai, K. Effect of microbial combination with organic fertilizer on *Elymus dahuricus*. *Open Geosci.* **2021**, *13*, 233–244. [CrossRef]
40. Zhu, Y.N.; Lou, Y.B.; Wang, W.L.; Liu, J.L.; Guo, M.M.; Kang, H.L.; Feng, L.Q.; Li, R.D. Effects of three plant root systems on rill erosion characteristics on coal dump slopes under simulated experiments. *Int. J. Sediment Res.* **2025**, *40*, 718–728. [CrossRef]
41. Huang, J.-K.; Dai, J.-P.; Scarpa, F.; Wang, Y.-Q.; Ji, J.-N.; Mao, Z. Random Root Distribution Affects the Mechanical Properties of the Soil-Root Composite and Root Reinforcement. *Catena* **2025**, *255*, 108896. [CrossRef]
42. Song, Y.; Li, R.; Zou, L.; Liu, Y.; Deng, Y.; Chen, Z.; Gao, W.; Wang, R. Roles of Attached Bacteria on the Growth and Metabolism of Microcystis aeruginosa with Limited Soluble Phosphorus. *ACS ES T Water* **2024**, *4*, 453–465. [CrossRef]
43. Issah, G.; Schoenau, J.J.; Lardner, H.A.; Knight, J.D. Nitrogen Fixation and Resource Partitioning in Alfalfa (*Medicago sativa* L.), Cicer Milkvetch (*Astragalus cicer* L.) and Sainfoin (*Onobrychis viciifolia* Scop.) Using ^{15}N Enrichment under Controlled Environment Conditions. *Agronomy* **2020**, *10*, 1438. [CrossRef]
44. Wu, T.; Bao, Y.; Su, Y.C.; Yang, T.D.; Leng, X.Y.; Shi, C.F. Impact of compound organic fertilizer-plant combined remediation on microbial community structure in mine tailings substrates. *Toxics* **2026**, *14*, 285. [CrossRef] [PubMed]

45. Lin, Q.; Yang, P.; Zhang, Y.; Zhang, W.; Wu, H. Metagenomic insights into coal slag remediation effects on soil and microbial health in Qinghai's Muli Coal Mine. *Microorganisms* **2024**, *12*, 2222. [CrossRef] [PubMed]
46. Yu, Z.; Yao, X.; Yang, M.; Hu, S.; An, X.; Li, C. Co-application of sheep manure and commercial organic fertilizer enhances plant productivity and soil quality in alpine mining areas. *Front. Microbiol.* **2024**, *15*, 1488121. [CrossRef] [PubMed]
47. *NY/T 3082-2017*; Determination of Chlorophyll Content in Fruits, Vegetables and Derived Products—Spectrophotometry Method. Ministry of Agriculture and Rural Affairs: Beijing, China, 2017. (In Chinese)
48. Kome, G.K.; Enang, R.K.; Yerima, B.P.K.; Lontsi, M.G.R. Models relating soil pH measurements in H_2O, KCl and $CaCl_2$ for volcanic ash soils of Cameroon. *Geoderma Reg.* **2018**, *14*, e00185. [CrossRef]
49. Zhang, L.; Xu, M.G.; Liu, Y.; Zhang, F.S.; Hodge, A.; Feng, G. Carbon and phosphorus exchange may enable cooperation between an arbuscular mycorrhizal fungus and a phosphate-solubilizing bacterium. *New Phytol.* **2016**, *210*, 1022–1032. [CrossRef] [PubMed]
50. Vitti, C.; Stellacci, A.M.; Leogrande, R.; Mastrangelo, M.; Cazzato, E.; Ventrella, D. Assessment of organic carbon in soils: A comparison between the Springer-Klee wet digestion and the dry combustion methods in Mediterranean soils (Southern Italy). *Catena* **2016**, *137*, 113–119. [CrossRef]
51. Van Bemmelen, J.M. Über die Bestimmung des Wassers, des Humus, des Schwefels, der in den colloïdalen Silikaten gebundenen Kieselsäure, des Mangans u. s. w. im Ackerboden. *Die Landwirthschaftlichen Vers.-Station.* **1890**, *37*, 279–290. (In German)
52. Douglas, L.A.; Riazi, A.; Smith, C.J. A semi-micro method for determining total nitrogen in soils and plant material containing nitrite and nitrate. *Soil Sci. Soc. Am. J.* **1980**, *44*, 431–433. [CrossRef]
53. Chen, B.; Yang, H.; Song, W.; Liu, C.; Xu, J.; Zhao, W.; Zhou, Z. Effect of N fertilization rate on soil alkali hydrolyzable N, subtending leaf N concentration, fiber yield, and quality of cotton. *Crop J.* **2016**, *4*, 323–330. [CrossRef]
54. Chen, Y.; Jia, J.; Wu, C.; Ramirez-Granada, L.; Li, G. Estimation on total phosphorus of agriculture soil in China: A new sight with comparison of model learning methods. *J. Soils Sediments* **2023**, *23*, 998–1007. [CrossRef]
55. Wang, C.Q.; Wang, Z.Y.; Huang, D.M.; Huang, Q.C.; Chen, Y.; Zhang, H.; Shui, Z.H. Recovery and recycling core of phosphogypsum: Characteristic hazardous elements risk assessment and analysis. *Process Saf. Environ. Prot.* **2023**, *170*, 738–756. [CrossRef]
56. Chinnasamy, S.; Bhatnagar, A.; Claxton, R.; Das, K.C. Biomass and bioenergy production potential of microalgae consortium in open and closed bioreactors using untreated carpet industry effluent as growth medium. *Bioresour. Technol.* **2010**, *101*, 6751–6760. [CrossRef] [PubMed]
57. Abdelfattah, A.; Ali, S.S.; Ramadan, H.; El-Aswar, E.I.; Eltawab, R.; Ho, S.-H.; Elsamahy, T.; Li, S.; El-Sheekh, M.M.; Schagerl, M.; et al. Microalgae-based wastewater treatment: Mechanisms, challenges, recent advances, and future prospects. *Environ. Sci. Ecotechnol.* **2023**, *13*, 100205. [CrossRef] [PubMed]
58. Zerveas, S.; Mente, M.S.; Tsakiri, D.; Kotzabasis, K. Microalgal photosynthesis induces alkalization of aquatic environment as a result of H^+ uptake independently from CO_2 concentration—New perspectives for environmental applications. *J. Environ. Manag.* **2021**, *289*, 112546. [CrossRef] [PubMed]
59. Gao, K. Approaches and involved principles to control pH/pCO_2 stability in algal cultures. *J. Appl. Phycol.* **2021**, *33*, 3497–3505. [CrossRef]
60. Hodgskiss, L.H.; Nagy, J.; Barnhart, E.P.; Cunningham, A.B.; Fields, M.W. Cultivation of a native alga for biomass and biofuel accumulation in coal bed methane production water. *Algal Res.* **2016**, *19*, 63–68. [CrossRef]
61. White, S.; Anandraj, A.; Bux, F. PAM fluorometry as a tool to assess microalgal nutrient stress and monitor cellular neutral lipids. *Bioresour. Technol.* **2011**, *102*, 1675–1682. [CrossRef] [PubMed]
62. Touloupakis, E.; Zittelli, G.C.; Benavides, A.M.S.; Torzillo, G. Growth and photosynthetic performance of *Nostoc linckia* (formerly *N. calcicola*) cells grown in BG11 and BG110 media. *Photochem. Photobiol. Sci.* **2022**, *22*, 795–807. [CrossRef] [PubMed]
63. Cassier-Chauvat, C.; Chauvat, F. Responses to Oxidative and Heavy Metal Stresses in Cyanobacteria: Recent Advances. *Int. J. Mol. Sci.* **2015**, *16*, 871–886. [CrossRef] [PubMed]
64. Lourembam, J.; Haobam, B.; Singh, K.B.; Verma, S.; Rajan, J.P. The molecular insights of cyanobacterial bioremediations of heavy metals: The current and the future challenges. *Front. Microbiol.* **2024**, *15*, 1450992. [CrossRef] [PubMed]
65. Usmonkulova, A.; Shonakhunov, T.; Kadirova, G.K. Activity of nitrogen-fixing cyanobacteria under salinity and heavy metals stress. *J. Pharm. Negat. Results* **2022**, *13*, 355–363. [CrossRef]
66. Pavlov, V.A.; Grigorenko, A.V.; Kovalenko, E.M.; Vavilkina, M.E.; Vlaskin, M.S. Effect of Initial Biomass Concentration on the Growth Kinetics of *Chlorella vulgaris* in Cylindrical Photobioreactors. *Bioengineering* **2026**, *13*, 804. [CrossRef] [PubMed]
67. Zhang, C.; Huang, X.; Chu, Y.; Ren, N.; Ho, S.-H. An overlooked effect induced by surface modification: Different molecular response of *Chlorella pyrenoidosa* to graphitized and oxidized nanodiamonds. *Environ. Sci. Nano* **2020**, *7*, 2302–2312. [CrossRef]
68. Paliwal, C.; Gebauer, R.; Mishra, S. Surviving the long fast: Biochemical and photosynthetic acclimation of *Synechocystis* sp. CCNM 2501 to chronic nitrogen and phosphorus starvation. *Front. Mar. Sci.* **2026**, *13*, 1925472. [CrossRef]

69. Vera-Vives, A.M.; Michelberger, T.; Morosinotto, T.; Perin, G. Assessment of photosynthetic activity in dense microalgae cultures using oxygen production. *Plant Physiol. Biochem.* **2024**, *208*, 108510. [CrossRef] [PubMed]
70. Madsen, M.A.; Semerdzhiev, S.; Twigg, J.D.; Moss, C.; Bavington, C.D.; Amtmann, A. Environmental modulation of exopolysaccharide production in the cyanobacterium Synechocystis 6803. *Appl. Microbiol. Biotechnol.* **2023**, *107*, 6121–6134. [CrossRef] [PubMed]
71. Moia, I.C.; Pereira, S.B.; Domizio, P.; De Philippis, R.; Adessi, A. *Phormidium ambiguum* and *Leptolyngbya ohadii* Exopolysaccharides under Low Water Availability. *Polymers* **2023**, *15*, 1889. [CrossRef] [PubMed]
72. Sun, Y.; Huang, Y.; Liao, Q.; Fu, Q.; Zhu, X. Enhancement of microalgae production by embedding hollow light guides to a flat-plate photobioreactor. *Bioresour. Technol.* **2016**, *207*, 31–38. [CrossRef] [PubMed]
73. Songserm, R.; Nishiyama, Y.; Sanevas, N. Light influences the growth, pigment synthesis, photosynthesis capacity, and antioxidant activities in *Scenedesmus falcatus*. *Scientifica* **2024**, *10*, 1898624. [CrossRef] [PubMed]
74. Maltsev, Y.; Maltseva, K.; Kulikovskiy, M.; Maltseva, S. Influence of light conditions on microalgae growth and content of lipids, carotenoids, and fatty acid composition. *Biology* **2021**, *10*, 1060. [CrossRef] [PubMed]
75. Milia, M.; Andreotti, V.; Giglioli, A.; Pasquini, V.; Addis, P.; Angioni, A. Use of Enriched Mine Water to Grow the Cyanobacterium *Arthrospira platensis* in Photobioreactors. *Foods* **2025**, *14*, 1665. [CrossRef] [PubMed]
76. Chen, L.; Gin, K.Y.; He, Y. Effects of sulfate on microcystin production, photosynthesis, and oxidative stress in Microcystis aeruginosa. *Environ. Sci. Pollut. Res. Int.* **2016**, *23*, 3586–3595. [CrossRef] [PubMed]
77. Sun, C.; Tan, S.; Qiu, Z.; Sun, S.; Jiang, P.; Chen, L. Effects of Different Exogenous Organic Substrates on Soil Carbon and Nitrogen Mineralization and Their Priming Effects. *Agronomy* **2023**, *13*, 3017. [CrossRef]
78. Kheirfam, H.; Sadeghi, S.H.; Homaee, M.; Zarei Darki, B. Quality Improvement of an Erosion-Prone Soil through Microbial Enrichment. *Soil Tillage Res.* **2017**, *165*, 230–238. [CrossRef]
79. Muñoz-Rojas, M.; Román, J.R.; Roncero-Ramos, B.; Erickson, T.E.; Merritt, D.J.; Aguilar, A.; Cantón, Y. Cyanobacteria Inoculation Enhances Carbon Sequestration in Soil Substrates Used in Dryland Restoration. *Sci. Total Environ.* **2018**, *636*, 1149–1154. [CrossRef] [PubMed]
80. Cao, B.; Zhang, Z.; Tong, Y.; Wang, Q.; Li, W.; Wei, C.; Zang, C.; Wang, W. Optimizing Cyanobacterial Biomass for Soil Restoration: Nutrient Enrichment and Microbial Modulation in Degraded Grasslands of Hulun Lake. *Bull. Environ. Contam. Toxicol.* **2025**, *114*, 75. [CrossRef] [PubMed]
81. Alvarez, A.L.; Weyers, S.L.; Gardner, R.D. Cyanobacteria-Based Soil Amendments in the Soil-Plant System: Effects of Inoculations on Soil Nutrient and Microbial Dynamics under Spring Wheat Growth. *Algal Res.* **2024**, *77*, 103326. [CrossRef]
82. Liang, X.; Zhu, Y.; Liu, H.; Xie, Z.; Li, G.; Li, D.; Liang, Y.; Peng, C. Nitrogen-Fixing Cyanobacteria Enhance Microbial Carbon Utilization by Modulating the Microbial Community Composition in Paddy Soils of the Mollisols Region. *Sci. Total Environ.* **2024**, *929*, 172609. [CrossRef] [PubMed]
83. Filip, Z.; Bielek, P. Susceptibility of Humic Acids from Soils with Various Contents of Metals to Microbial Utilization and Transformation. *Biol. Fertil. Soils* **2002**, *36*, 426–433. [CrossRef]
84. Muhammad, S.; Shaukat, M.; Yasin, M.; Mahmood, A.; Javaid, M.M.; Al-Sadoon, M.K.; Głowacka, A.; Ahmed, M.A.A. Compost and Humic Acid Amendments Are a Practicable Solution to Rehabilitate Weak Arid Soil for Higher Winter Field Pea Production. *Sci. Rep.* **2023**, *13*, 17519. [CrossRef] [PubMed]
85. Ngearnpat, N.; Tiche, S.; Wongkantrakorn, N.; Duangjan, K.; Phinyo, K.; Issakul, K. Functional Differentiation of Indigenous Nostocalean Cyanobacteria: Effects of Biomass and Extracellular Polymeric Substances on Rice Growth and Soil Properties. *Crops* **2026**, *6*, 40. [CrossRef]
86. Crouzet, O.; Consentino, L.; Pétraud, J.-P.; Marrauld, C.; Aguer, J.-P.; Bureau, S.; Le Bourvellec, C.; Touloumet, L.; Bérard, A. Soil Photosynthetic Microbial Communities Mediate Aggregate Stability: Influence of Cropping Systems and Herbicide Use in an Agricultural Soil. *Front. Microbiol.* **2019**, *10*, 1319. [CrossRef] [PubMed]
87. Chen, Y.; Sun, K.; Yang, Y.; Gao, B.; Zheng, H. Effects of Biochar on the Accumulation of Necromass-Derived Carbon, the Physical Protection and Microbial Mineralization of Soil Organic Carbon. *Crit. Rev. Environ. Sci. Technol.* **2024**, *54*, 39–67. [CrossRef]
88. Fang, J.; Chen, B.; Wang, F.; Li, W.; Zhang, H.; Fang, J.; Liu, S.; Zheng, Z.; Guo, M.; Niu, S. Nitrogen, Phosphorus, and Potassium Co-Limitation in Terrestrial Ecosystems: A Global Meta-Analysis. *Plants People Planet.* **2024**, *6*, 1329–1340. [CrossRef]
89. Zhao, B.; Jia, X.; Yu, N.; Murray, J.D.; Yi, K.; Wang, E. Microbe-Dependent and Independent Nitrogen and Phosphate Acquisition and Regulation in Plants. *New Phytol.* **2024**, *242*, 1507–1522. [CrossRef] [PubMed]
90. Jacinavicius, F.R.; Pacheco, A.B.F.; Chow, F.; Verissimo da Costa, G.C.; Kalume, D.E.; Rigonato, J.; Schmidt, E.C.; Sant'Anna, C.L. Different Ecophysiological and Structural Strategies of Toxic and Non-Toxic Microcystis Aeruginosa (Cyanobacteria) Strains Assessed under Culture Conditions. *Algal Res.* **2019**, *41*, 101548. [CrossRef]
91. Mukherjee, C.; Chowdhury, R.; Ray, K. Phosphorus Recycling from an Unexplored Source by Polyphosphate Accumulating Microalgae and Cyanobacteria—A Step to Phosphorus Security in Agriculture. *Front. Microbiol.* **2015**, *6*, 1421. [CrossRef] [PubMed]

92. Plouviez, M.; Brown, N. Polyphosphate Accumulation in Microalgae and Cyanobacteria: Recent Advances and Opportunities for Phosphorus Upcycling. *Curr. Opin. Biotechnol.* **2024**, *90*, 103207. [CrossRef] [PubMed]
93. Feng, B.; Ma, J.; Liu, Y.; Zhang, X.; Chen, Y.; Weng, L. Research Progress on Nitrogen Transport and Transformation in Farmland Soils. *J. Agric. Resour. Environ.* **2025**, *42*, 277–287. (In Chinese)
94. Toribio, M.; Iglesias, M.P.; Correndo, A.; Wyngaard, N.; Reussi Calvo, N. Determinants of Ammonia Volatilization Losses and Their Effect on Maize Yield. *Cienc. del Suelo* **2023**, *41*, 193–205.
95. Iqbal, A.; Iqbal, M.; Alamzeb, M.; Meizhen, S.; Xiling, Z.; Arif, M.; Du, X.; Lichtfouse, E. (Eds.) *Sustainable Agriculture Reviews 58: Phosphorus Use Efficiency for Sustainable Agriculture*; Springer: Cham, Switzerland, 2022.
96. Díaz-Pérez, F.J.; Díaz, R.; Valdés, G.; Valdebenito-Rolack, E.; Hansen, F. Effects of Microalgae and Compost on the Yield of Cauliflower Grown in Low Nutrient Soil. *Chil. J. Agric. Res.* **2023**, *83*, 181–194. [CrossRef]
97. Sun, Z.; Liu, X.; Ugya, A.Y.; Liu, H.; Sun, L.; Luo, G. Microalgae and Cyanobacteria as a Tool for Agricultural Sustainability: A Review of Biofertilizer and Biostimulant Potential. *Front. Plant Sci.* **2026**, *16*, 1733394. [CrossRef] [PubMed]
98. Zhao, Y.; Fu, C.; Liu, Y.; Xiang, D.; Wang, Z.; Qin, H.; Cheng, C.; Li, Q. Effects of Adding Microalgae and Cow Manure Organic Fertilizer on Soil Chemical Properties and Bacterial Community, Yield and Quality of Flue-Cured Tobacco. *J. Yunnan Agric. Univ. (Nat. Sci.)* **2024**, *39*, 172–181. (In Chinese)
99. Song, X.; Liu, J.; Feng, Y.; Zhou, C.; Li, X.; Yan, X.; Ruan, R.; Cheng, P. Microalgae-Based Biofertilizers Improve Fertility and Microbial Community Structures in the Soil of Potted Tomato. *Front. Plant Sci.* **2024**, *15*, 1461945. [CrossRef] [PubMed]
100. Gu, B.; Wang, R.; Wang, S.; Zhang, Y.; Han, X.; Zhu, B.; Dijkstra, F.A.; Jiang, Y. Microbial Immobilization Shapes the Non-Linear Response of Allochthonous Nitrogen Retention to Grassland Acidification Within Soil Aggregates. *Glob. Change Biol.* **2025**, *31*, e70229. [CrossRef] [PubMed]
101. Charteris, A.F.; Knowles, T.D.J.; Mead, A.; Reay, M.K.; Michaelides, K.; Evershed, R.P. The Differential Assimilation of Nitrogen Fertilizer Compounds by Soil Microorganisms. *FEMS Microbiol. Lett.* **2024**, *371*, fnae041. [CrossRef] [PubMed]
102. Fenn, L.B.; Kissel, D.E. Ammonia Volatilization from Surface Applications of Ammonium Compounds on Calcareous Soils: I. General Theory. *Soil Sci. Soc. Am. J.* **1973**, *37*, 855–859. [CrossRef]
103. Zou, X.; Cheng, J.; Cheng, J.; Jiang, X.; Huang, B.; Zhou, T.; Chen, L. Effects of Microalgae (Chlorella ZJ and *Anabaena azotica*) Application on Soil Carbon and Nitrogen Fractions in a Degraded Purple Soil: A Laboratory Incubation Study. *Sustainability* **2026**, *18*, 4057. [CrossRef]
104. Yang, W.; Jia, Y.; Yu, J.; Yang, J.; Gu, P.; Yan, Y.; Wang, K.; Jiao, Y. The Mechanisms Driving Ammonia Emission Variations in Alkaline Soil Under Different Irrigation and Fertilization Management Practices in Arid Regions. *Water Air Soil Pollut.* **2024**, *235*, 814. [CrossRef]
105. Khan, A.; Guo, S.; Wang, R.; Zhang, S.; Yang, X.; He, B.; Li, T. An Assessment of Various Pools of Organic Phosphorus Distributed in Soil Aggregates as Affected by Long-Term P Fertilization Regimes. *Soil Use Manag.* **2023**, *39*, 833–848. [CrossRef]
106. Gan, X.; Janus, J.; Willbold, S.; Dombinov, V.; Kuhn, A.J.; Amelung, W.; Reinecke, D.; Calahan, D.; Nedbal, L.; Klose, H.; et al. Wheat Growth and Phosphorus Uptake from Polyculture Algal Biofilms Are Synergistically Modulated by Arbuscular Mycorrhizal Fungi and *Serendipita vermifera*. *Plant Soil* **2025**, *514*, 1923–1940. [CrossRef]
107. Sakhraoui, A.; Ltaeif, H.B.; Sakhraoui, A.; Villalba, J.J.; Castillo, J.M.; Rouz, S. Sainfoin (*Onobrychis viciifolia*) a Legume with Great Ecological and Agronomical Potential under Climate Change. *J. Agric. Sci.* **2024**, *162*, 307–331. [CrossRef]
108. Knight, C.C. Simulated Residual Nitrogen Scavenging and Recovery among Cover Crop Systems Using Nitrogen-15 in a Corn Production Setting. Master's Thesis, Mississippi State University, Mississippi State, MS, USA, 2024.
109. Asha, J.F.; Ahmed, S.F.; Biswas, A.; Bony, Z.F.; Chowdhury, M.R.; Sarker, B.C. Impacts of Long-Term Irrigation with Coalmine Effluent Contaminated Water on Trace Metal Contamination of Topsoil and Potato Tubers in Dinajpur Area, Bangladesh. *Heliyon* **2024**, *10*, e24100. [CrossRef] [PubMed]
110. Abad-Valle, P.; Álvarez-Ayuso, E.; Murciego, A.; Muñoz-Centeno, L.M.; Alonso-Rojo, P.; Villar-Alonso, P. Arsenic Distribution in a Pasture Area Impacted by Past Mining Activities. *Ecotoxicol. Environ. Saf.* **2018**, *147*, 228–237. [CrossRef] [PubMed]
111. Zhang, Q.; Wang, X.; Zhang, Z.; Liu, H.; Liu, Y.; Feng, Y.; Yang, G.; Ren, C.; Han, X. Linking Soil Bacterial Community Assembly with the Composition of Organic Carbon during Forest Succession. *Soil Biol. Biochem.* **2022**, *173*, 108790. [CrossRef]
112. Ho, A.; Di Lonardo, D.P.; Bodelier, P.L.E. Revisiting Life Strategy Concepts in Environmental Microbial Ecology. *FEMS Microbiol. Ecol.* **2017**, *93*, fix006. [CrossRef] [PubMed]
113. Fierer, N.; Bradford, M.A.; Jackson, R.B. Toward an Ecological Classification of Soil Bacteria. *Ecology* **2007**, *88*, 1354–1364. [CrossRef] [PubMed]
114. Zhang, Q.-C.; Shamsi, I.H.; Xu, D.-T.; Wang, G.-H.; Lin, X.-Y.; Jilani, G.; Hussain, N.; Chaudhry, A.N. Chemical Fertilizer and Organic Manure Inputs in Soil Exhibit a Vice Versa Pattern of Microbial Community Structure. *Appl. Soil Ecol.* **2012**, *57*, 1–8. [CrossRef]
115. -Stone, B.; Dijkstra, P.; Finley, B.; Fitzpatrick, R.; Foley, M.M.; Hayer, M.; Hofmockel, K.S.; Koch, B.J.; Li, J.; Liu, X.J.; et al. Life history strategies among soil bacteria—Dichotomy for few, continuum for many. *ISME J.* **2023**, *17*, 611–619. [CrossRef] [PubMed]

116. Siedt, M.; Teggers, E.-M.; Linnemann, V.; Schäffer, A.; van Dongen, J.T. Microbial Degradation of Plant Residues Rapidly Causes Long-Lasting Hypoxia in Soil upon Irrigation and Affects Leaching of Nitrogen and Metals. *Soil Syst*. **2023**, *7*, 62. [CrossRef]
117. Ludwig, W.; Euzéby, J.; Schumann, P.; Busse, H.-J.; Trujillo, M.E.; Kämpfer, P.; Whitman, W.B. Road Map of the Phylum Actinobacteria. In *Bergey's Manual of Systematic Bacteriology*, 2nd ed.; Goodfellow, M., Kämpfer, P., Busse, H.-J., Trujillo, M.E., Suzuki, K., Ludwig, W., Whitman, W.B., Eds.; Springer: New York, NY, USA, 2012; Volume 5, pp. 1–28.
118. Lewin, G.R.; Carlos, C.; Chevrette, M.G.; Horn, H.A.; McDonald, B.R.; Stankey, R.J.; Fox, B.G.; Currie, C.R. Evolution and Ecology of Actinobacteria and Their Bioenergy Applications. *Annu. Rev. Microbiol*. **2016**, *70*, 235–254. [CrossRef] [PubMed]
119. Shih, P.M.; Ward, L.M.; Fischer, W.W. Evolution of the 3-Hydroxypropionate Bicycle and Recent Transfer of Anoxygenic Photosynthesis into the *Chloroflexi*. *Proc. Natl. Acad. Sci. USA* **2017**, *114*, 10749–10754. [CrossRef] [PubMed]

Disclaimer/Publisher's Note: The statements, opinions and data contained in all publications are solely those of the individual author(s) and contributor(s) and not of MDPI and/or the editor(s). MDPI and/or the editor(s) disclaim responsibility for any injury to people or property resulting from any ideas, methods, instructions or products referred to in the content.